Take the Short Route in Confidence Crises*

Carlos Bolivar
University of Minnesota

Teerat Wongrattanapiboon
University of Minnesota

May 31, 2026

Abstract

During the 2010–2012 European debt crisis, Italian sovereign spreads spiked far beyond what fundamentals could explain, while debt maturity shortened. Existing quantitative work attributes only a modest role to self-fulfilling risk. We develop a sovereign debt model with endogenous maturity and Calvo-style self-fulfilling crises in which long-term bonds carry within-period confidence risk and short-term debt insures against it. Maturity shortening is the optimal response to the increase in confidence risk, not evidence against it. A particle filter on Italian data attributes roughly 80 percent of the late-2011 spread spike to a rise in confidence risk, with direct implications for crisis interventions.

Keywords: Sovereign debt crises, self-fulfilling crises, debt maturity, confidence risk

JEL classification: F34, H63, G12, E62

*We thank Manuel Amador and Timothy J. Kehoe for all their continuous support, guidance, and helpful comments on various stages of the project. We also thank seminar participants of the trade workshop at the University of Minnesota for their comments.

1 Introduction

During the European sovereign debt crisis of 2010–2012, Italian sovereign spreads spiked, peaking above 500 basis points in late 2011. This rise prompted an active policy debate about its source. Several European policymakers argued that the spike could not be reconciled with the underlying macroeconomic deterioration, which was modest by comparison: output contracted during the 2008–2009 and 2011–2012 recessions, and debt-to-GDP rose by roughly 20 percentage points. They instead invoked a narrative of a "confidence crisis" to justify their interventions, arguing that pessimistic investor beliefs had become self-reinforcing: nervous investors demanded high interest rates, raising debt payments, compromising fiscal sustainability, and in turn reinforcing investors' initial fears. However, recent quantitative work has cast doubt on this view. Taking the canonical Cole–Kehoe model with endogenous maturity to Italian data, Bocola and Dovis (2019) attribute a modest effect of confidence risk on the spread, and as a result the model fails to account for the spike in spreads.

Theoretical work points to a different source of multiplicity in sovereign debt markets, one that operates through long-term bonds. Lorenzoni and Werning (2019) and Aguiar and Amador (2020) show types of multiplicity that emerge from the interaction between the price of long-bonds and the issuance. In this paper, we propose a Calvo-style framework in which Italy's decision to shorten debt maturity during the crisis is the optimal response to rising confidence risk associated with long-term bonds. As a result, short-term debt reduces the government's exposure to a confidence crisis in the short run, so a rising probability of a crisis tilts the optimal portfolio toward shorter bonds. Our main result is that self-fulfilling crises account for approximately 80 percent of the Italian spread at the late-2011 peak.

Our theory builds on Lorenzoni and Werning (2019), a Calvo-style framework in which self-fulfilling risk emerges from the pricing of long-term bonds. We enrich the benchmark model with an endogenous choice of debt maturity. A calibrated fiscal rule determines government spending before bond prices are realized, so the government's financing need is predetermined when investors bid. When the bad sunspot is realized, the long-term price collapses and the government must issue a larger quantity to clear the budget at the depressed price, retaining market access. The long-term bond therefore carries within-period confidence risk. Short-term bonds, by contrast, are not exposed to multiplicity. Their price reflects only the probability of default in the next period, so it is insulated from the effect of future borrowing, making them less exposed to multiple equilibria. In Cole–Kehoe rollover crises, the short-term bond is the risky one because it requires higher payments during exclusion, and long-term debt is the insurance instrument. In our framework, the prescription flips: higher confidence risk calls for shorter maturity.

This asymmetry creates a trade-off in the maturity choice. Shortening maturity today reduces the government's exposure to within-period confidence risk: less long-term debt must clear at the potentially adverse price. But more short-term debt today must be rolled over next period, raising next period's financing need and the residual long-term issuance required tomorrow. The optimal maturity decision balances today's insurance against tomorrow's exposure. When the probability of a confidence crisis rises, the value of today's insurance increases, tilting the optimal portfolio toward shorter maturities despite the higher future rollover cost.

We calibrate the model to features of Italy's economy prior to the crisis and use a particle filter to infer the sequence of unobserved shocks from the data during the crisis. Our framework distinguishes two confidence shocks: the probability of a crisis and its realization. The joint dynamics of maturity shortening and spread widening identify the path of confidence risk. Our model matches both observables for Italy during 2010–2012 and attributes the bulk of the late-2011 spread spike to an increase in confidence risk over the episode. These results have direct implications for the design and evaluation of crisis interventions and support the policies implemented by the ECB at the time.

Related Literature. Two traditions model self-fulfilling sovereign debt crises: Cole–Kehoe crises, where investors exclude the government from credit markets (Cole and Kehoe, 2000), and Calvo-style crises, where markets remain open but borrowing costs spike (Calvo, 1988; Lorenzoni and Werning, 2019). We adopt the Calvo approach, as it better captures the European experience where countries faced high yields but retained market access, and because the Calvo mechanism generates the opposite maturity prediction relative to Cole–Kehoe, which is central to our identification. Quantitative work has extended both branches: Conesa and Kehoe (2017) embed a Cole–Kehoe rollover mechanism in a model with endogenous fiscal effort and show that governments may rationally gamble for redemption, while Roch and Uhlig (2018) characterize how bailout guarantees pin down the fundamental equilibrium even when sunspots remain possible. On the Calvo side, Ayres et al. (2024) show that multiplicity is quantitatively relevant only during persistent stagnations; we complement their analysis by adding endogenous maturity choice, which provides identification of confidence shocks in the data. Aguiar et al. (2022) characterize self-fulfilling crises driven by lack of commitment at bond auctions, including "desperate deals" closely related to the bad equilibrium in our model. Auclert and Rognlie (2016) prove equilibrium is unique with one-period debt, confirming that long-term bonds are necessary for our multiplicity mechanism.

We build on the quantitative sovereign default framework: Eaton and Gersovitz (1981) and Arellano (2008) on default risk, Aguiar and Gopinath (2006) on the role of trend shocks, and

Chatterjee and Eyigungor (2012) on long-term debt with default. On maturity choice, Niepelt (2014) provides the canonical theoretical statement under lack of commitment: equilibrium maturity shortens during crises because short-term debt is less exposed to the time-inconsistency of future repayment. Broner et al. (2013) document the empirical counterpart in a panel of emerging economies, where issuance shifts toward short maturities when long-term risk premia spike. Arellano and Ramanarayanan (2012) and Hatchondo et al. (2016) study the insurance-dilution trade-off, and Bigio et al. (2023) characterize the optimal continuum-maturity issuance problem under liquidity costs. Aguiar et al. (2019) show the sovereign should actively manage only short-term debt under limited commitment. In our model, maturity plays a different role: it manages within-period confidence risk.

The most direct antecedent is Bocola and Dovis (2019), who find a modest role for confidence risk in Italian spreads using a Cole–Kehoe model with endogenous maturity; Bocola et al. (2019) survey the broader Eaton–Gersovitz approach to Eurozone debt and reach similar conclusions. In their Cole–Kehoe setup, higher rollover risk calls for *longer* maturity, so the same observed shortening signals low perceived risk and the quantitative weight of confidence is bounded by the rarity of observed exclusion. In our Calvo-style framework with long-term bond multiplicity, the prediction flips: higher confidence risk calls for *shorter* maturity, reconciling Italy's observed behavior with the confidence crisis narrative. On the empirical side, Bocola (2016) uses a related particle-filter approach to quantify sovereign-bank feedback during the Italian crisis; De Grauwe and Ji (2013) show that EMU bond yields decoupled from fiscal fundamentals after 2010; and Krishnamurthy et al. (2018) estimate large announcement effects of the SMP and OMT on Italian, Spanish, and Portuguese yields. Within the structural European crisis literature, Aguiar et al. (2015) study self-fulfilling crises in monetary unions, Bianchi and Mondragon (2022) show lack of monetary independence amplifies rollover risk, and Corsetti and Dedola (2016) analyze how central bank purchases eliminate the pessimistic equilibrium. Our model abstracts from sovereign-bank feedback, a channel that further amplifies the welfare relevance of confidence risk: Acharya et al. (2014) document the empirical transfer of risk from banks to sovereigns, Farhi and Tirole (2018) provide a theoretical foundation for the doom loop, and Brunnermeier et al. (2016) propose European Safe Bonds as a structural response. For broader surveys, see Aguiar and Amador (2014) and Aguiar et al. (2016).

Outline. The paper is organized as follows. Section 2 presents the model environment. Section 3 characterizes the government's problem and the recursive equilibrium. Section 4 studies the role of maturity structure in reducing confidence risk. Section 5 presents the calibration and examines the model's multiplicity properties. Section 6 applies a particle filter to Italian data to decompose sovereign spreads into fundamental and confidence components. Section 7 concludes.

2 Model

We consider a small open economy with discrete time and an infinite horizon. The periods are indexed by $t \in \{0, 1, 2, \ldots\}$. The economy is populated by a benevolent government and a continuum of risk-averse foreign investors.

2.1 Timing

We adopt the timing in Lorenzoni and Werning (2019). A fiscal rule pins down current expenditure before bond prices are realized, so the government cannot offset adverse price movements by cutting spending within the period. The government's only active choice is the next-period short-term debt $b_{S,t+1}$; long-term issuance is adjusted to clear the budget constraint. Within each period t, the sequence is as follows.

Figure 1: Timing

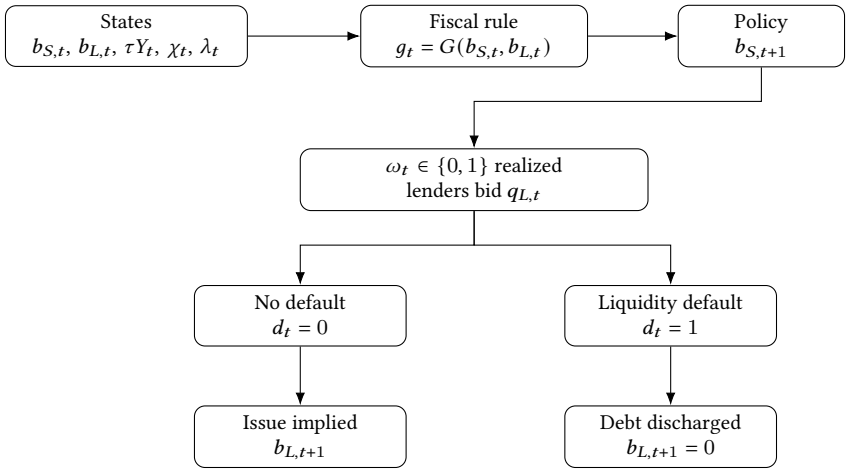

At the start of the period t, tax revenue τY_t (where Y_t is output and τ is a fixed tax rate), the term-premium shock χ_t, and the crisis-probability shock λ_t are realized. A fiscal rule $G(\cdot)$ then establishes current spending g_t as a function of the inherited debt portfolio. Given g_t, the government chooses the next-period of short-term debt $b_{S,t+1}$. Next, the sunspot $\omega_t \in \{0, 1\}$ is realized and lenders bid for long-term bonds, determining their price $q_{L,t}$. Finally, taking the price as given, the government issues whatever long-term debt $b_{L,t+1}$ clears the budget constraint. If no feasible issuance clears the budget, the government experiences a *liquidity default* ($d_t = 1$). Long-term issuance and default are equilibrium outcomes implied by $b_{S,t+1}$ and the price of the bond, rather than independent policy choices. After default, the government enters the period $t + 1$ with zero debt.

Compared to Lorenzoni and Werning (2019), the government here chooses a portfolio of short- and long-term bonds. As shown by Lorenzoni and Werning (2019) and Aguiar and Amador (2020), the interaction between current prices and future borrowing in long-term bonds can generate self-fulfilling crises. Lorenzoni and Werning (2019) also show that with only short-term debt, the government chooses short-term issuance $b_{S,t+1}$, which has a unique price and is immune to self-fulfilling dynamics. Long-term issuance $b_{L,t+1}$ then adjusts to clear the budget constraint and remains subject to the multiplicity of the Laffer curve. This portfolio choice allows the government to manage its exposure to confidence crises.

2.2 Stochastic Processes

We model two sources of uncertainty: *fundamental risk* and *confidence risk*. Fundamental risk is summarized by the vector of economic shocks $\{y_t, \chi_t\}$, where $y_t = \log(Y_t)$ is the logarithmic output and χ_t is a term-premium shock. The two shocks are correlated and evolve according to a joint VAR(1) process:

$$\begin{bmatrix} y_{t+1} \\ \chi_{t+1} \end{bmatrix} = \begin{bmatrix} (1-\rho_y)\mu_y \\ 0 \end{bmatrix} + \begin{bmatrix} \rho_y & 0 \\ 0 & \rho_\chi \end{bmatrix} \begin{bmatrix} y_t \\ \chi_t \end{bmatrix} + \begin{bmatrix} \epsilon^y_{t+1} \\ \epsilon^\chi_{t+1} \end{bmatrix},$$

where $[\epsilon^y, \epsilon^\chi]'$ are normally distributed with the covariance matrix Σ.

The confidence risk reflects the possibility of multiple equilibria in financial markets. The probability of a confidence crisis, λ_t, evolves as an AR(1) process:

$$\lambda_{t+1} = (1-\rho_\lambda)\bar{\lambda} + \rho_\lambda \lambda_t + \sigma_\lambda \varepsilon^\lambda_{t+1}, \qquad \varepsilon^\lambda \sim N(0,1),$$

where $\bar{\lambda}$ is the long-run mean. The continuous process is discretized onto a bounded grid $[0, \lambda_{\max}]$ (see Appendix B). After the government chooses $b_{S,t+1}$ but before lenders bid for long-term bonds, a sunspot $\omega_t \in \{0,1\}$ is realized independently: with probability λ_t the bad sunspot occurs ($\omega_t = 1$) and bond prices are low; with probability $1-\lambda_t$ the good sunspot occurs ($\omega_t = 0$) and bond prices are high. Thus, λ_t captures *time-varying vulnerability* to a confidence crisis, while ω_t captures the *realized* equilibrium selection within the period.

2.3 Government

We express the model in terms of fiscal variables, as in Bocola and Dovis (2019), so that the primitives governing default risk, tax revenue, spending commitments, and debt service map directly to observable fiscal data.

Preferences. The government has time-separable preferences over public expenditures:

$$\mathbb{E}_0 \sum_{t=0}^{\infty} \beta^t \frac{g_t^{1-\sigma}}{1-\sigma}, \tag{1}$$

where $\beta \in (0,1)$ is the discount factor, σ is the risk-aversion parameter, and $\mathbb{E}_t$ denotes expectations conditional on the information available at time t.

Fiscal rule. Government spending in period t follows a calibrated fiscal rule:

$$g_t = G(b_{S,t}, b_{L,t}) \equiv \bar{g} - \alpha_1 \max\left(b_{S,t} + b_{L,t} - \bar{b},\ 0\right), \tag{2}$$

where $\bar{g}$ is the average expenditure, $\bar{b}$ is a reference debt level, and $\alpha_1 \geq 0$ governs fiscal tightening when total debt exceeds $\bar{b}$. The specification captures the empirical regularity that governments tighten fiscal policy when debt is elevated (Bohn, 1998).

The fiscal rule plays two roles. First, it determines the government's financing need before the sunspot is drawn: because g_t is a known function of the state at the start of the period, the deficit $g_t - \tau Y_t$ is predetermined when lenders bid for long-term bonds. This preserves the friction of Lorenzoni and Werning (2019): the government cannot escape a bad equilibrium by committing to lower spending within the period. Second, we choose $(\bar{g}, \alpha_1, \bar{b})$ jointly to generate plausible unconditional moments and to preserve Laffer-curve multiplicity at Italian debt levels. This multiplicity is the structural requirement that drives our identification.

Debt instruments. As in Arellano and Ramanarayanan (2012), the government issues short- and long-term bonds. The short-term bond pays $(1+\kappa_S)$ per unit of face value at maturity, where $\kappa_S > 0$ is a fixed coupon, and its price is $q_{S,t}$. Following Hatchondo et al. (2016), long-term bonds have geometrically declining coupons: one unit issued at t implies an infinite stream of payments starting at $t+1$,

$$\kappa_L,\ (1-\delta)\kappa_L,\ (1-\delta)^2\kappa_L,\ \ldots, \tag{3}$$

where $\kappa_L > 0$ and $\delta \in (0,1)$.[1] Long-term debt evolves according to

$$b_{L,t+1} = (1-\delta)b_{L,t} + i_t, \tag{4}$$

[1] We set κ_S and κ_L to target bond prices of 1 at par in the absence of default risk. With a stochastic discount factor, this is an approximation: coupons are calibrated using the unconditional mean discount factor as the risk-free rate, $\kappa_S = \bar{R}_f - 1$ and $\kappa_L = \delta + \bar{R}_f - 1$, where $\bar{R}_f \equiv \mathbb{E}[M_{t,t+1}]^{-1}$. This normalization is standard in the quantitative sovereign debt literature (Arellano and Ramanarayanan, 2012; Hatchondo et al., 2016).

where $b_{L,t}$ denotes the outstanding stock at t, i_t is new issuance in period t, and the long-term bond price is $q_{L,t}$.

Fiscal budget. The government enters period t with portfolio $\{b_{S,t}, b_{L,t}\}$, spending g_t determined by the fiscal rule (2), and tax revenue τY_t. Under repayment ($d_t = 0$), the period budget constraint is

$$g_t + (1 + \kappa_S)b_{S,t} + \kappa_L b_{L,t} = \tau Y_t + q_{S,t}\, b_{S,t+1} + q_{L,t}\big(b_{L,t+1} - (1 - \delta)b_{L,t}\big). \tag{5}$$

Spending and debt service are financed with taxes and new issuance of short- and long-term debt.

Default and recovery. We assume the government repays whenever feasible, so default occurs only when tax revenue and market financing are insufficient to satisfy the budget constraint. Let $d_t = 1$ denote default and $d_t = 0$ repayment. Under default, public spending falls to an exogenous level $g_D < \tau Y_{\min}$, where $Y_{\min}$ is the minimum realization of output.[2] Following default, all bondholders receive a recovery value equal to a fraction ϕ of the government's net fiscal surplus, distributed pari passu across the outstanding debt stock:

$$\tilde{\nu}_{t+1} \equiv \frac{\phi(\tau Y_{t+1} - g_D)}{b_{S,t+1} + b_{L,t+1}}. \tag{6}$$

Both short- and long-term bondholders receive $\tilde{\nu}_{t+1}$ per unit of face value in default, capped at the face value of each instrument. This specification makes default costly through the reduction in public spending and the capital loss on long-term claims. The defaulting government regains access to financial markets immediately in the following period, entering with a clean balance sheet: $b_{S,t+1} = b_{L,t+1} = 0$.[3]

[2] Bocola and Dovis (2019) and Chatterjee and Eyigungor (2012) specify a state-dependent output cost of default, $d_t = \max\{0, d_0 Y_t + d_1 Y_t^2\}$, which makes default more painful at high output levels and raises the government's debt capacity in simulation. We use the constant spending floor g_D because the fiscal rule already raises debt capacity by committing to austerity as debt rises, making a state-dependent default cost redundant. The recovery pool $\phi(\tau Y - g_D)$ retains state dependence through Y, preserving cyclicality in the effective cost of default.

[3] Most quantitative sovereign debt models assume stochastic exclusion from capital markets following default (Arellano, 2008; Hatchondo et al., 2016; Bocola and Dovis, 2019). We assume immediate re-entry for two reasons. First, Italy never defaulted during our sample period, making a prolonged exclusion period counterfactual for our empirical application. Second, the self-fulfilling mechanism operates within the period, through the sunspot and Laffer-curve equilibrium selection, so the duration of post-default exclusion does not affect this friction.

2.4 International Investors

International investors are competitive and price government bonds using a stochastic discount factor (SDF) $M_{t,t+1}$. Following Bocola and Dovis (2019), we model changes in risk aversion as a fundamental shock that is observable, exogenous, and common across countries, capturing global risk appetite rather than country-specific confidence dynamics.[4] In particular, we model the lenders' SDF as

$$M_{t,t+1} = \exp\{m_{t,t+1}\}, \tag{7}$$

$$m_{t,t+1} = -(\phi_0 + \phi_1 \chi_t) \; - \; \frac{1}{2}\kappa_t^2 \; + \; \kappa_t \, \varepsilon_{\chi,t+1}, \tag{8}$$

$$\chi_{t+1} = \rho_\chi \chi_t + \varepsilon_{\chi,t+1}, \qquad \varepsilon_{\chi,t+1} \sim \mathcal{N}(0,1), \tag{9}$$

$$\kappa_t = \kappa_0 + \kappa_1 \chi_t. \tag{10}$$

Short-term debt. Bond prices satisfy standard no-arbitrage conditions. Short-term bonds receive recovery $\tilde{\nu}_{t+1}$ per unit in default (the same rate as long-term bonds), so their price satisfies

$$q_{S,t} = \mathbb{E}_t \Big[M_{t,t+1} \Big((1 - d_{t+1})(1 + \kappa_S) + d_{t+1} \, \tilde{\nu}_{t+1} \Big) \Big]. \tag{11}$$

Long-term debt. Conditional on repayment, one unit pays the coupon κ_L next period and leaves a fraction $(1 - \delta)$ of the claim outstanding, which trades at $q_{L,t+1}$. Under default, the bond receives $\tilde{\nu}_{t+1}$ per unit of face value. Therefore,

$$q_{L,t} = \mathbb{E}_t \left[M_{t,t+1} \left((1 - d_{t+1}) \big(\kappa_L + (1 - \delta) q_{L,t+1} \big) + d_{t+1} \tilde{\nu}_{t+1} \right) \right]. \tag{12}$$

Expectations in (11)–(12) integrate over both fundamental shocks and equilibrium selection in financial markets, so confidence risk affects bond prices through the distribution of future default and continuation values.

[4] This specification follows Ang and Piazzesi (2003) and is used by Bocola and Dovis (2019) to allow for time-variation in risk premia on longer-maturity bonds.

2.5 Competitive Equilibrium

Definition 1 (Competitive Equilibrium)**.** Given initial government debt $\{b_{S,0}, b_{L,0}\}$, the fiscal rule $G(\cdot)$, the government's short-term debt policy $\{b_{S,t+1}\}_{t=0}^{\infty}$, and the exogenous processes $\{Y_t,\ \chi_t,\ \lambda_t,\ \omega_t\}_{t=0}^{\infty}$, a *competitive equilibrium* is a sequence of bond prices, long-term issuance, and default outcomes $\{q_{S,t},\ q_{L,t},\ b_{L,t+1},\ d_t\}_{t=0}^{\infty}$ such that:

i *Default.* Default in period t occurs if and only if no feasible $b_{L,t+1} \geq 0$ satisfies the budget constraint (5) at the prevailing price $q_{L,t}$: $d_t = 1\{\text{no feasible } b_{L,t+1} \text{ exists}\}$. When multiple feasible $b_{L,t+1}$ exist, the sunspot $\omega_t \in \{0, 1\}$ selects between them.

ii *Bond pricing.* Conditional on the equilibrium default and issuance outcomes, bond prices satisfy (11) and (12), where recovery $\tilde{v}_{t+1}$ is determined by (6) given the equilibrium debt portfolio $(b_{S,t+1}, b_{L,t+1})$.

iii *Market clearing.* In each period, bond markets clear: the quantities of short- and long-term claims held by investors equal the quantities issued by the government, $\{b_{S,t+1}, b_{L,t+1}\}$.

The model delivers two predictions that distinguish it from the Cole–Kehoe framework underlying Bocola and Dovis (2019). First, the long-term bond price $q_{L,t}$ depends on λ_t even when $\omega_t = 0$, because lenders price the elevated probability of the bad equilibrium one period ahead. Second, the government's optimal portfolio response to a rise in λ_t is to substitute toward short-term debt, shortening the maturity of the portfolio. Section 5 calibrates the model to Italian data, and Section 6 uses these two predictions jointly: spreads and the maturity choice each carry information on λ, and together they identify the sequence of confidence shocks behind the 2010–2012 episode.

3 Government Problem

We restrict attention to a Markov environment with payoff-relevant state (s, λ), where

$$s \equiv (b_S, b_L, y, \chi)$$

collects the inherited debt portfolio (b_S, b_L), the output shock y, and the term-premium shock χ, and λ is the time-varying probability of the bad equilibrium. The government's only choice variable is next-period short-term debt b'_S. The fiscal rule $G(b_S, b_L)$ pins spending g. Long-term

issuance b'_L and default d are equilibrium outcomes: given b'_S, default occurs if no feasible b'_L clears the budget at the prevailing price, and conditional on repayment, b'_L is the issuance that clears the budget. When multiple budget-clearing values exist, the sunspot $\omega \in \{0, 1\}$ selects between them: $\omega = 0$ picks the good equilibrium (high price, low issuance) and $\omega = 1$ the bad equilibrium (low price, high issuance). We conjecture bond price schedules (Q_S, Q_L), verified in Section 3.4, and derive all equilibrium objects as functions of these prices.

3.1 The Laffer Curve

We conjecture that bond price schedules $Q_S(y, \chi, \lambda, b'_S, b'_L)$ and $Q_L(y, \chi, \lambda, b'_S, b'_L)$ exist. Bond prices depend on the current fundamental shocks (y, χ) and confidence risk λ, but *not* on the current debt portfolio (b_S, b_L). Once the government commits to new issuance (b'_S, b'_L), lenders' expected payoffs depend only on current fundamentals and the forward-looking quantities that flow from (b'_S, b'_L). Because λ follows a persistent AR(1) process, the current λ affects the distribution of next-period λ' and therefore enters bond prices. Given these price schedules, define the government's net financial revenue from issuing (b'_S, b'_L) as

$$\mathcal{L}(s, \lambda, b'_S, b'_L) = Q_L(y, \chi, \lambda, b'_S, b'_L)\big(b'_L - (1-\delta)b_L\big) + Q_S(y, \chi, \lambda, b'_S)\, b'_S - (1+\kappa_S)b_S - \kappa_L b_L. \quad (13)$$

Note that Q_S in the Laffer curve does not depend on the candidate b'_L being evaluated. Because short-term bonds are sold before the sunspot ω is drawn, lenders price them at the λ-weighted average across both equilibrium outcomes: $Q_S(y, \chi, \lambda, b'_S) = (1-\lambda)\, Q_S(y, \chi, \lambda, b'_S, b^*_{L,g}) + \lambda\, Q_S(y, \chi, \lambda, b'_S, b^*_{L,b})$, where $(b^*_{L,g}, b^*_{L,b})$ are the equilibrium long-term debt levels. This defines a fixed point: the pre-sunspot price $Q_S(\cdot)$ depends on $(b^*_{L,g}, b^*_{L,b})$, which in turn depend on Q_S through the Laffer curve. We solve this fixed point jointly in the value-function iteration of Appendix B: at each iteration the previous-iteration Q_S is used to evaluate the Laffer curve and identify $(b^*_{L,g}, b^*_{L,b})$, and the new Q_S is computed as the λ-weighted average over these equilibrium roots. By contrast, Q_L is evaluated at each candidate b'_L because long-term bonds are priced simultaneously with the sunspot selection.

As $b'_L \to \infty$, default becomes certain and the per-unit bond price approaches the discounted recovery value: $Q_L \to \mathbb{E}[M(\chi')\,\phi(\tau Y' - g_D)/b'_L]$. Total long-term revenue $Q_L(b'_L - (1-\delta)b_L)$ therefore converges to the discounted recovery pool $\mathbb{E}[M(\chi')\,\phi(\tau Y' - g_D)]$. Define the *Laffer asymptote*

$$\mathcal{L}_\infty(s, \lambda, b'_S) \;\equiv\; \mathbb{E}\big[M(\chi')\,\phi(\tau Y' - g_D)\big] + Q_S(y, \chi, \lambda, b'_S)\, b'_S - (1+\kappa_S)\, b_S - \kappa_L\, b_L, \quad (14)$$

which is the maximum net revenue the government can raise from the bond market in the limit of unlimited long-term issuance. When $\mathcal{L}_\infty < g - \tau Y$, no high-issuance level of long-term borrowing can clear the budget if the bad sunspot ($\omega = 1$) is realized.

3.2 Default and Issuance Rules

An equilibrium requires a value of b'_L at which $\mathcal{L}(s, \lambda, b'_S, b'_L) = g - \tau Y$. Following Lorenzoni and Werning (2019), only intersections on locally *increasing* portions of $\mathcal{L}$ are stable equilibria; intersections on decreasing portions are unstable and discarded. Let

$$\mathbb{B}^+_L(s, \lambda, b'_S) = \left\{ b'_L : \mathcal{L}(s, \lambda, b'_S, b'_L) = g - \tau Y, \quad \tfrac{\partial \mathcal{L}}{\partial b'_L} > 0 \right\} \tag{15}$$

denote the set of stable budget-clearing levels.

Default depends on the sunspot realization ω. Under the good sunspot ($\omega = 0$), default occurs only under fundamental insolvency: when no stable clearing level exists. Under the bad sunspot ($\omega = 1$), default additionally occurs when the Laffer asymptote falls short of the deficit, $\mathcal{L}_\infty(s, \lambda, b'_S) < g - \tau Y$, so that no high-issuance equilibrium exists (Cole–Kehoe style). Formally,

$$D(s, \lambda, \omega, b'_S) = \begin{cases} 1, & \omega = 0 \text{ and } \mathbb{B}^+_L(s, \lambda, b'_S) = \emptyset, \\ 1, & \omega = 1 \text{ and } \left[\mathbb{B}^+_L(s, \lambda, b'_S) = \emptyset \text{ or } \mathcal{L}_\infty(s, \lambda, b'_S) < g - \tau Y\right], \\ 0, & \text{otherwise.} \end{cases} \tag{16}$$

The second case captures two outcomes. Fundamental default occurs when $\mathbb{B}^+_L = \emptyset$, so neither sunspot can clear the budget. Cole–Kehoe default occurs when a unique low-issuance equilibrium exists for $\omega = 0$ but the discounted recovery pool is insufficient to finance the deficit even at the limit of long-term issuance, leaving the bad sunspot without a stable clearing root.

Given $\mathbb{B}^+_L(s, \lambda, b'_S)$, the sunspot selects among stable clearing levels: $\omega = 0$ picks the lowest (good equilibrium, high price/low issuance) and $\omega = 1$ picks the highest (bad equilibrium, low price/high issuance). The equilibrium long-term debt rule is

$$B_L(s, \lambda, \omega, b'_S) = \begin{cases} \max \mathbb{B}^+_L(s, \lambda, b'_S), & \text{if } \omega = 1 \text{ and } D(s, \lambda, 1, b'_S) = 0, \\ \min \mathbb{B}^+_L(s, \lambda, b'_S), & \text{if } \omega = 0 \text{ and } D(s, \lambda, 0, b'_S) = 0, \\ 0, & \text{if } D(s, \lambda, \omega, b'_S) = 1. \end{cases} \tag{17}$$

Our timing implies that short- and long-term instruments play asymmetric roles in equilib-

rium selection. Multiplicity arises when $\mathbb{B}_L^+(s, \lambda, b'_S)$ contains more than one element: multiple stable long-term issuance levels clear the budget, and the sunspot selects between them. By contrast, short-term debt is priced by international investors and, given government policies and the default rule, its price is uniquely pinned down. This asymmetry makes long-term issuance the margin that generates confidence-driven fluctuations in prices, while the government can use short-term issuance to reduce confidence risk.

3.3 Value Function

Given the rules for default and long-term debt, the value function of the government solves

$$V(s, \lambda) = \max_{b'_S} \mathbb{E}_{y', \chi', \lambda', \omega} \Big[(1-d)\big(u(g) + \beta V(b'_S, b'_L, y', \chi', \lambda')\big) + d\big(u(g_D) + \beta V(0, 0, y', \chi', \lambda')\big) \Big], \tag{18}$$

$$\text{s.t.} \qquad d = D(s, \lambda, \omega, b'_S), \qquad b'_L = B_L(s, \lambda, \omega, b'_S).$$

Equation (18) states that the government chooses b'_S taking prices as given; default d and long-term debt b'_L are implied by budget feasibility and the equilibrium long-term bond price. The period payoff is $u(g)$ under repayment and $u(g_D)$ under default, and the next-period state resets to zero debt after default, consistent with the timing of Sections 2 and 3. The solution yields a decision rule for short-term debt,

$$b'_S = \mathcal{B}_S(s, \lambda).$$

Following Dvorkin et al. (2021), we introduce i.i.d. taste shocks to the portfolio choice, replacing the hard argmax with a logit-smoothed distribution over the b'_S grid. Appendix B details the full specification and solution algorithm.

3.4 Price Functions

In a Markov equilibrium, the conjectured bond price schedules must satisfy competitive investors' no-arbitrage conditions, given the equilibrium law of motion implied by government policies and the default and issuance rules. Using the SDF $M(\chi)$, bond prices satisfy:

$$Q_S(y, \chi, \lambda, b'_S, b'_L) = \mathbb{E}\Big[M(\chi, \chi') \Big((1-d')(1+\kappa_S) + d' \, \tilde{v}' \Big) \Big], \tag{19}$$

$$Q_L(y, \chi, \lambda, b'_S, b'_L) = \mathbb{E}\Big[M(\chi, \chi') \Big\{ (1-d')\big(\kappa_L + (1-\delta) Q_L(y', \chi', \lambda', b''_S, b''_L)\big) + d' \, \tilde{v}' \Big\} \Big], \tag{20}$$

where $d' = D(s', \lambda', \omega', b''_S)$, $b''_S = \mathcal{B}_S(s', \lambda')$, $b''_L = B_L(s', \lambda', \omega', b''_S)$, and $s' = (b'_S, b'_L, y', \chi')$. The continuation bond price $Q_L(y', \chi', \lambda', b''_S, b''_L)$ is evaluated at next-period fundamentals (y', χ', λ') and the portfolio (b''_S, b''_L) chosen at s'. Both Q_S and Q_L are conditional on no current-period default: under $d = 1$ the government enters autarky with zero issuance and these prices are not invoked. Lenders therefore price bonds off the next-period default indicator d', the only default event that can affect their realized payoff.

Although ω does not appear directly as an argument of Q_L, the realized price in equilibrium is $Q_L(y, \chi, \lambda, b'_S, B_L(s, \lambda, \omega, b'_S))$, which inherits ω-dependence through the issuance rule B_L. The two-way feedback between bond prices and issuance makes multiple equilibria possible: a low price forces more long-term issuance to clear the budget, which raises default risk and justifies the low price; a high price requires less issuance, which lowers default risk and justifies the high price. The sunspot selects which self-consistent equilibrium is realized: under $\omega = 0$, the good equilibrium (low issuance, high price); under $\omega = 1$, the bad equilibrium (high issuance, low price).

3.5 Markov Equilibrium

Definition 2 (Markov Perfect Equilibrium)**.** Given an initial state s_0, the laws of motion for (y, χ, λ), the sunspot distribution $\omega \mid \lambda$, and the fiscal rule $G(\cdot)$, a Markov perfect equilibrium consists of functions

$$V,\ \mathcal{B}_S,\ D,\ B_L,\ Q_S,\ Q_L$$

such that:

i) **Feasibility and selection**: Default is given by (16), and conditional on repayment, long-term debt satisfies (17).

ii) **Government optimality**: Given (Q_S, Q_L) and the induced mappings D and B_L, V solves the Bellman equation (18) and $\mathcal{B}_S$ is the associated optimal policy rule.

iii) **Pricing**: Given $(\mathcal{B}_S, D, B_L)$, bond prices satisfy the no-arbitrage conditions (19)–(20).

In equilibrium, government portfolio choices are optimal given prices, prices are consistent with competitive pricing given policies, and the sunspot selects among long-term issuance levels that clear the fiscal budget when multiplicity arises. Section 4 characterizes when $\mathbb{B}^+_L(s, \lambda, b'_S)$ contains multiple elements and shows that raising b'_S contracts this set, eliminating the bad equilibrium.

4 Multiplicity and the Laffer Curve

When confidence risk rises, the government substitutes toward short-term debt to reduce its within-period exposure to a low long-term bond price. Confidence risk operates through the pricing of long-term bonds at settlement, so shifting financing toward short-term issuance shrinks the volume of long-term debt that must clear at potentially adverse prices. Section 4.1 characterizes the set of states for which multiplicity arises, and Section 4.2 shows how short-term debt shifts the boundaries of this set.

4.1 Multiplicity

We begin by characterizing the multiplicity region as a function of the state and the government's portfolio choice. Figure 2 illustrates a typical shape for the Laffer curve, $\mathcal{L}(b'_L;\, s, \lambda, b'_S)$, defined in equation (13). The curve captures the net revenue the government can raise from the bond market as a function of its long-term issuance b'_L, given the state (s, λ) and its short-term debt choice b'_S.

Figure 2: Laffer curve at a state with two stable equilibria

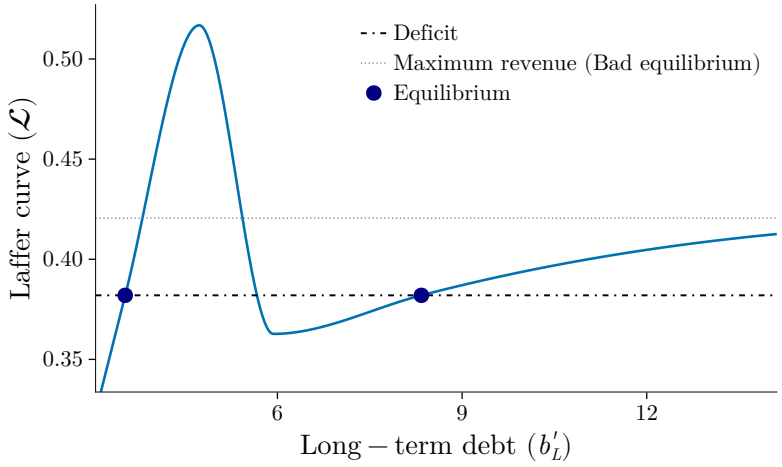

Notes: The Laffer curve $\mathcal{L}(b'_L; s, \lambda, b'_S)$ as a function of long-term issuance b'_L. Dash-dotted line: financing need $g - \tau Y$. Dotted line: maximum revenue $\mathcal{L}_\infty$, the asymptote of the recovery branch (see equation (14)). Open circle: good equilibrium ($\omega = 0$); filled circle: bad equilibrium ($\omega = 1$).

The non-monotonic shape of the Laffer curve reflects the tension between two forces. On the one hand, issuing more long-term debt mechanically raises revenue: the *quantity effect*. On the other hand, higher issuance worsens rollover risk, depressing bond prices and reducing the revenue per unit issued: the *price effect*. On the upward-sloping portion of the curve, the quantity

effect dominates: markets are unconcerned about default, prices remain high, and more debt means more revenue. Beyond a threshold, the price effect takes over: bond prices collapse faster than the debt stock grows, and total revenue falls even as the face value of debt increases. As in Lorenzoni and Werning (2019), the interaction between these two forces generates the non-monotonic shape shown in Figure 2.

The second upward-sloping portion of the Laffer curve, at high b'_L, reflects the dilution of existing creditors' recovery claims. The recovery pool $\phi(\tau Y' - g_D)$ is shared pari passu across all outstanding debt, so per-unit recovery is $\phi(\tau Y' - g_D)/(b'_S + b'_L)$. As new issuance grows, current-period issuance $b'_L - (1-\delta)b_L$ captures a larger share of this fixed pool, generating a second increasing region in $\mathcal{L}$ even though the total pool is unchanged. It is this second branch that sustains the bad (high-issuance) equilibrium in the Lorenzoni–Werning sense.

This structure allows for multiple equilibria. An equilibrium requires the government's net market revenue to equal its financing need, $g - \tau Y$. Graphically, an equilibrium is an intersection between the Laffer curve and the horizontal line at height $g - \tau Y$. For a range of deficits, multiple stable intersections coexist.

Let $\mathbb{B}^+_L(s, \lambda, b'_S)$ denote the set of stable budget-clearing long-term issuance levels defined in (15). The state-policy space partitions into three regions, distinguished by how many stable equilibria exist and whether the bad sunspot triggers default. In the **safe region** $\mathcal{M}_S$, one stable equilibrium sits on the low-issuance branch and the bad sunspot does not default; equilibrium features low long-term debt and high bond prices, with ω irrelevant. In the **Multiplicity - Run region** $\mathcal{M}_R$, one stable good equilibrium exists but the Laffer curve lies below the deficit at all high issuance levels, so the bad sunspot cannot clear the budget and defaults immediately, in the spirit of Cole and Kehoe (2000). In the **Multiplicity - Low price region** $\mathcal{M}_M$, two stable equilibria coexist: one with low issuance and high prices, the other with high issuance and low prices, with the sunspot ω selecting between them via the Lorenzoni and Werning (2019) mechanism. Formally:

Definition 3 (Equilibrium regions)**.**

$$\begin{aligned}
\mathcal{M}_S &\equiv \{(s, \lambda, b'_S) : |\mathbb{B}^+_L(s, \lambda, b'_S)| = 1, \quad D(s, \lambda, 1, b'_S) = 0\}, \\
\mathcal{M}_R &\equiv \{(s, \lambda, b'_S) : \mathbb{B}^+_L(s, \lambda, b'_S) \neq \emptyset, \quad D(s, \lambda, 1, b'_S) = 1\}, \\
\mathcal{M}_{LP} &\equiv \{(s, \lambda, b'_S) : |\mathbb{B}^+_L(s, \lambda, b'_S)| = 2\}.
\end{aligned}$$

Since bond prices depend on the current λ (which forecasts future crisis risk), the boundaries of all three regions shift with λ. Output operates analogously: higher y simultaneously reduces the financing need $g - \tau Y$ and increases the prices of bonds through improved expected repayment,

two strengthening forces that push the economy towards the safe region $\mathcal{M}_S$.

4.2 Short-term debt and confidence risk

The government can shift the boundaries of the multiplicity region by changing its short-term issuance b'_S. Financing a larger share of the deficit through short-term bonds reduces the amount the government must raise through long-term issuance at settlement. This makes it easier to clear the budget even if long-term bond prices drop, and therefore makes the bad equilibrium harder to sustain. Increasing b'_S thus shrinks the multiplicity region today, but the additional short-term debt must be rolled over next period, raising future rollover pressure and potentially widening the future multiplicity region. The government's maturity decision rests on this trade-off, and our quantitative analysis traces this balance through Italy's 2010–2012 episode. When the probability of a confidence crisis (λ) increases, the insurance value of short-term debt increases, inclining the optimal portfolio towards shorter maturities despite the higher rollover cost.

We formalize this mechanism in a stylized infinite-horizon environment. The stylized environment isolates the insurance channel and allows an analytical characterization of the conditions under which short-term debt mitigates confidence risk. The general result, with the corresponding conditions for the full model, is stated in Appendix A.

A stylized environment. Consider an infinite-horizon version of the model in which the output and the term-premium shock are constant, $Y_t = \bar{Y}$ and $\chi_t = \bar{\chi}$, and the confidence-risk probability is a constant parameter $\lambda \in (0, 1)$. The fiscal rule, the default rule, and the recovery rule are unchanged. We further assume that the period utility is linear $u(g) = g$, so that the marginal value of consumption is constant: the long-bond stock does not raise the marginal cost of carrying short-term debt, and the within-period insurance channel of b'_S operates without a competing precautionary motive. We restrict attention to a stationary equilibrium in which the government chooses a constant short-term issuance b^*_S each period, the long-debt level alternates between two values b^g_L and b^b_L according to the realized sunspot, and the bond prices at the two equilibrium roots, Q_S, Q^g_L and Q^b_L, are constants determined by stationary fixed-point conditions. The bad-sunspot root sits on the recovery branch of the Laffer curve; the good-sunspot root is repaid this period, and the bond's one-period-ahead payoff is a λ-weighted average of its good-state and bad-state values:

$$Q^b_L = \tilde{\nu} \equiv \frac{\phi(\tau\bar{Y} - g_D)}{b^*_S + b^b_L}, \tag{21}$$

$$Q^g_L = \beta\big[(1-\lambda)\big(\kappa_L + (1-\delta)Q^g_L\big) + \lambda\,\tilde{\nu}\big]. \tag{22}$$

The price of the short-bond Q_S is quoted at the auction, before ω is drawn. The bond matures one period later, paying $1+\kappa_S$ if the government repays and the per-unit recovery $\tilde{v}$ if it defaults. With $\omega = 1$ triggering the bad-equilibrium outcome on the recovery floor, the short-bond price satisfies

$$Q_S \;=\; \beta\big[(1-\lambda)(1+\kappa_S) + \lambda\,\tilde{v}\big]. \tag{23}$$

Proposition 1 (Insurance value of short-term debt, stylized environment)**.** *In the stylized stationary equilibrium, suppose that the primitives satisfy*

$$\beta\kappa_L \;>\; \tilde{v}\big[1-\beta(1-\delta)\big],$$

Then the optimal short-term issuance is strictly increasing in confidence risk,

$$\frac{\partial b_S^*}{\partial \lambda} \;>\; 0.$$

Proof. See Appendix A. □

In this environment, the long bond is worth more in the good sunspot than in the bad one: its good-state price is Q_L^g, while in the bad state it only trades at its recovery value $Q_L^b = \tilde{v}$. The reason is that, in a good sunspot, the bond is fully serviced: it pays a coupon κ_L every period, and a fraction $1-\delta$ of the principal survives and can be sold again at the same price next period. Intuitively, the investor is holding a perpetuity that keeps generating payments and retains resale value, so the bond is valuable. In contrast, in a bad sunspot the bond is marked down to its recovery value $\tilde{v}$: investors expect to get only this reduced amount back, so the bond is strictly less valuable.

As the perceived risk λ of the bad sunspot rises, investors attach more weight to this low recovery value and less to full repayment. This makes the good-state price $Q_L^g(\lambda)$ drift downward toward $\tilde{v}$: even in the good sunspot, people price the bond more cautiously because they increasingly anticipate the possibility of ending up in the bad sunspot.

This gap in values gives short-term debt an insurance role. From the government's budget identity, issuing one more unit of short-term debt allows the government to buy back Q_S/Q_L^ω units of long-term debt in sunspot state ω. Because the long bond is cheaper in the bad sunspot ($Q_L^b = \tilde{v} < Q_L^g$), each unit of short-term debt lets the government issue less long-term debt precisely in the bad state, when the long-bond market is weakest and long-term borrowing is most costly.

The mechanism therefore depends on two ingredients of the calibration. The first is the re-

striction of the primitive parameters in Proposition 1 on the long-bond coupon, the discount factor, the decay rate, and the recovery value. The second is a moderate cross partial derivative of the continuation value. The general statement of the result for the full model with stochastic shocks and endogenous prices, together with the conditions for the result to extend, is in the Appendix A.

5 Quantitative Analysis

We calibrate the model to match long-run averages of the Italian economy, taking the SDF, term-premium-process, and discount-factor parameters directly from Bocola and Dovis (2019) for comparability. We first describe the calibration, then verify that the calibrated model exhibits Laffer-curve multiplicity at Italian debt levels, and document the government's optimal maturity response to rising crisis probability. Finally, we use the calibrated model to decompose Italian sovereign spreads during the 2010–2012 crisis.

5.1 Calibration

Our calibration targets three long-run Italian moments: the average debt-to-GDP ratio, the average sovereign spread, and the average debt maturity. The fiscal-rule parameters $(\bar{g}, \alpha_1, \bar{b})$, the recovery rate ϕ, the default-period spending g_D, and the confidence-risk process parameters $(\lambda_{\max}, \rho_\lambda)$ are jointly calibrated by minimizing the GMM distance between the simulated and empirical moments, subject to the structural side-restriction that the calibrated state admits the Laffer-curve multiplicity at Italian debt levels (discussed below). We fix the remaining parameters at conventional values or directly empirical counterparts.

The baseline parameters are in Table 1. The utility curvature parameter is $\sigma = 2$, a standard value in macroeconomic models. The long-term bond decay is $\delta = 0.033$, implying an average duration of 7.6 years. The tax rate is $\tau = 0.41$, matching the average tax revenue–to-GDP ratio in Italy.

The fiscal rule parameters $(\bar{g}, \alpha_1, \bar{b})$ require special treatment because they serve two functions simultaneously. First, they must generate plausible unconditional fiscal dynamics: $\bar{g}$ is the long-term spending level the rule prescribes at the reference debt level $\bar{b}$, and α_1 governs the speed of fiscal consolidation in response to debt deviations. Second, α_1 must be small enough that the calibrated state lies in $\mathcal{S}_M$ or $\mathcal{S}_{CK}$ (defined in Section 4) at debt levels representative of Italy during 2008–2012. This second requirement is structural rather than statistical: if α_1 is too large, the fiscal rule commits to such deep austerity that the deficit can always be financed at the good equilibrium

regardless of the sunspot realization, eliminating the multiplicity that drives our results. We therefore choose $(\bar{g}, \alpha_1, \bar{b})$ jointly to satisfy both requirements and verify that the calibrated values place the modal Italian state in $\mathcal{S}_M$ or $\mathcal{S}_{CK}$ (the filter that recovers this state is introduced in Section 6).

Table 1: Model Parameters

Parameter	**Symbol**	**Value**	**Target / Source**
Predetermined parameters			
Risk aversion	σ	2	Conventional value
Long-term bond decay	δ	0.033	Long-term bond duration ($\approx$ 7.6 years)
Tax rate	τ	0.41	Italian tax revenues / GDP
Discount factor	β	0.98	Bocola and Dovis (2019)
GDP process			
GDP persistence	ρ_y	0.9668	Italian GDP (detrended)
GDP mean	μ_y	-0.0002	Italian GDP (detrended)
GDP std. dev.	σ_y	0.008	Italian GDP (detrended)
SDF and term-premium process (taken from Bocola and Dovis 2019)			
SDF intercept	ϕ_0	0.005	Bocola and Dovis (2019)
SDF slope	ϕ_1	0.002	Bocola and Dovis (2019)
Price-of-risk intercept	κ_0	0.161	Bocola and Dovis (2019)
Price-of-risk slope	κ_1	0.374	Bocola and Dovis (2019)
Term-premium persistence	ρ_χ	0.513	Bocola and Dovis (2019)
Term-premium std. dev.	σ_χ	1.0	Bocola and Dovis (2019)
Calibrated via method of simulated moments			
Recovery rate	ϕ	0.50	Method of simulated moments
Default spending	g_D	0.013	Method of simulated moments
Average spending	$\bar{g}$	0.46	Method of simulated moments
Fiscal austerity slope	α_1	0.09	Method of simulated moments
Reference debt level	$\bar{b}$	2.8	Method of simulated moments
Crisis prob. upper bound	$\lambda_{\max}$	0.08	Method of simulated moments
Crisis prob. persistence	ρ_λ	0.5	Method of simulated moments

We estimate the GDP-process parameters from detrended Italian GDP data. We take the parameters of SDF, term-premium-process, and discount-factor from Bocola and Dovis (2019). In particular, we set $\beta = 0.98$ following Bocola and Dovis 2019 and verify that model moments are insensitive to this value: because default in our model is a liquidity event determined by clearing the bond market rather than a strategic choice, β does not govern the default threshold as does in strategic default models. We calibrate the fiscal-rule parameters $(\bar{g}, \alpha_1, \bar{b})$ as described above, not from a regression but to satisfy both the moment targets and the multiplicity requirement at

Italian debt levels. The recovery rate ϕ, the spending in the default-period g_D, and the confidence-risk limits $(\lambda_{\min}, \lambda_{\max}, \rho_\lambda)$ are calibrated to meet three empirical targets: the average debt-to-GDP ratio, the average sovereign spread and the average debt maturity. Appendix C provides empirical definitions of these variables.

Table 2: Empirical Targets: Data vs. Model

Moment	**Data**	**Model**
Average debt-to-GDP ratio (%)	87.9	92.9
Average spread (basis points)	61	76.7
Average debt maturity (years)	6.8	6.89

The model matches the average maturity within a month (6.89 vs. 6.8 years), produces a debt-to-GDP ratio of 92.9 percent against 87.9 in the data, and a spread of 77 bp against 61 in the data. We balance unconditional moment fit against filter fit in Section 6: calibrations that more tightly match the unconditional moments produce worse filter fits during the 2010–2012 crisis episode.

Verification of Proposition 1 on the filtered path. We evaluate the four sufficient conditions of Proposition 2 (the full-model statement) in each filtered Italian quarter (2008:Q2–2012:Q2). Condition (i) holds strictly at every quarter: the second finite difference of $\mathcal{V}$ in b'_L is strictly negative, ranging from -1.4 to -2.9. Condition (ii) holds strictly: $\partial\mathcal{L}/\partial b'_S$ lies in $[0.90, 1.00]$, close to its theoretical upper bound of $1 + \kappa_S$. Conditions (iii) and (iv) hold for every particle for which the underlying state lies in the multiplicity region. The bad-sunspot realization $\omega = 1$ is rare in posterior mass (essentially zero in every quarter), consistent with Italy not defaulting on the sample.

5.2 Short-Term Debt and Multiplicity

At Italy's median estimated debt state, increasing short-term issuance from low to high levels eliminates the bad-equilibrium intersection of the Laffer curve (Figure 3). With low short-term debt (solid blue), the deficit line intersects the Laffer curve at two stable points: the good equilibrium (low issuance, high price, open circle) and the bad equilibrium (high issuance, low price, filled circle). With high short-term debt (dashed orange), only one stable intersection survives. By financing a larger share of the deficit through short-term bonds, whose price is predetermined before the sunspot ω is drawn, the government reduces the long-term issuance required to clear the budget at settlement, making the bad equilibrium infeasible. This is the quantitative counterpart of the mechanism formalized in Proposition 1.

Figure 3: Short-term debt and equilibrium multiplicity

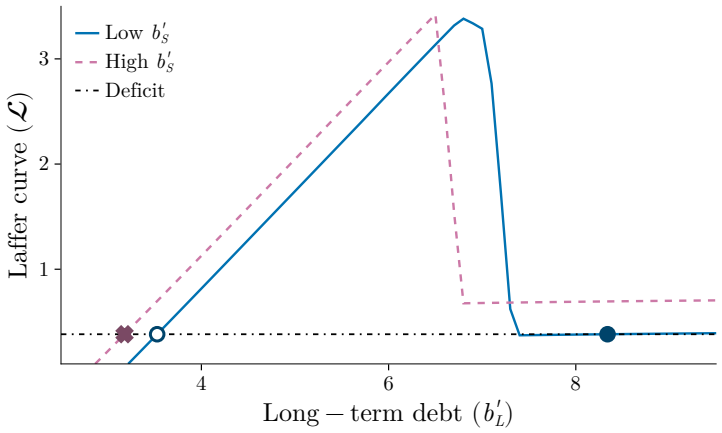

Notes: The Laffer curve $\mathcal{L}(b'_L; s, \lambda, b'_S)$ is plotted at Italy's median estimated debt portfolio (recovered by the particle filter) for two levels of short-term debt b'_S. Stable budget-clearing intersections are marked with an open circle (good equilibrium) and a filled circle (bad equilibrium) for the low b'_S curve (blue, solid). The high b'_S curve (orange, dashed) has a unique equilibrium marked with a cross.

5.3 Optimal Maturity Response

Short-term debt issuance rises with confidence risk λ at all output levels (Figure 4). The government consistently shortens its debt maturity as λ rises, consistent with Proposition 1.

Figure 4: Short-term debt policy: response to rising crisis probability

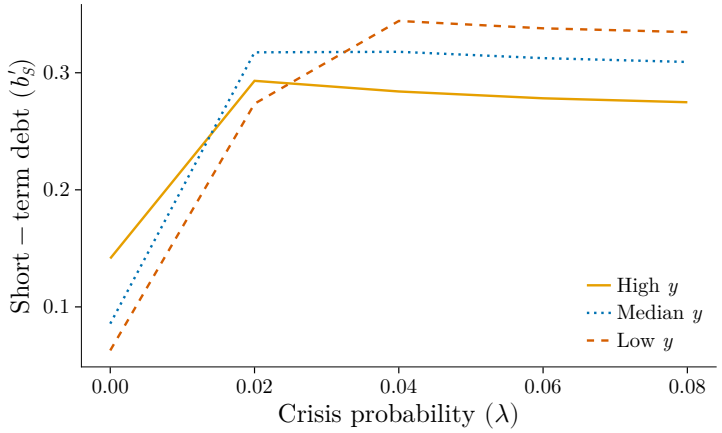

Notes: Expected short-term debt $\mathrm{E}[b'_S \mid s, \lambda]$ as a function of crisis probability λ, for three output levels (high, median, low y) at the representative calibrated debt state.

The response exhibits a level reversal across output. At low λ, the government issues the most short-term debt when output is high, reflecting greater fiscal capacity to absorb rollover costs. As λ rises, the ranking inverts: states with lower output issue more short-term debt at

high λ. Weaker fundamentals place the government closer to the multiplicity threshold, making the option value of eliminating the bad equilibrium larger. The low-output line ends highest at large λ: the insurance motive is strongest for the weakest fundamentals.

All three lines flatten early: high y by $\lambda \approx 0.02$, the remaining two by $\lambda \approx 0.04$, well below the grid maximum of $\lambda = 0.08$. This matches Proposition 1, which holds conditional on $\mathcal{S}_M$. Once b'_S is high enough to push the Laffer trough above the deficit line, the bad equilibrium disappears and the state transitions to $\mathcal{S}_U$. Further increases in λ beyond that point bring no additional insurance benefit, so the marginal incentive to raise b'_S vanishes.

The insurance motive binds most strongly at intermediate and high b_L, where the multiplicity regions are the widest (Figure 5). We map the multiplicity landscape in the (b'_S, b_L) space at the representative output and debt state, for two levels of probability of a crisis λ. The background color indicates which Laffer-curve case the government faces at each state-policy pair: green for the Safe region, blue for the Multiplicity-Run region (Cole–Kehoe), and pink for the Multiplicity-Low-price region (Lorenzoni–Werning). The black curve traces $\mathrm{E}[b'_S \mid b_L, \lambda]$: the expected short-term issuance the government chooses at each level of long-term debt b_L.

Figure 5: Multiplicity landscape and optimal short-term debt policy

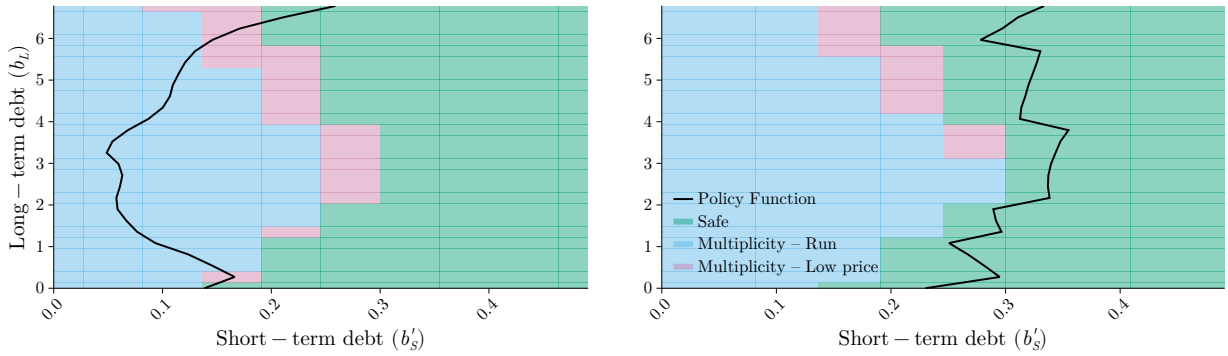

(a) No confidence risk ($\lambda = 0$)

(b) High confidence risk ($\lambda = 0.08$)

Notes: Background colors indicate the Laffer-curve case at each state-policy pair (b'_S, b_L): green = Safe; blue = Multiplicity – Run (Cole–Kehoe); pink = Multiplicity – Low price (Lorenzoni–Werning). The black curve is $\mathrm{E}[b'_S \mid b_L, \lambda]$, the expected short-term debt the government chooses given the inherited long-term debt state b_L. All other state variables held at Italy's median estimated debt portfolio.

Two features stand out. First, the Safe region (green) lies to the right: choosing a sufficiently high b'_S pushes the economy out of both multiplicity regions regardless of b_L. This is the quantitative counterpart of Proposition 1: short-term debt reducers risk of self-fulfilling crises by reducing the residual long-term issuance that must be cleared at adverse prices. Second, the policy curve shifts rightward as λ increases from 0 to 0.08: the government chooses more short-term debt to move into the Safe region. The shift is greatest at intermediate and high levels of b_L, where the

multiplicity regions are the broadest and the insurance value of the maturity shortening is the highest.

6 Decomposing Italian Spreads

We now apply the model to interpret the 2008–2012 Italian sovereign debt crisis. Following Bocola and Dovis (2019), we cast the model as a non-linear state-space system and use a Sequential Monte Carlo particle filter to estimate the unobserved states. The fundamental side of our filter matches theirs: output and the term premium directly identify fundamental risk. The difference lies in confidence: our Calvo-style mechanism allows crises without default. Our timing also makes maturity shortening a signal of increased risk of confidence, reversing the identification in Bocola and Dovis (2019).

6.1 The State-Space Representation

The observation and transition equations are

$$X_t = h(S_t) + \eta_t,$$
$$S_t = f(S_{t-1}, \epsilon_t),$$

where the functions h and f are defined by the model's equilibrium conditions and policy functions, and η_t is a vector of measurement errors.

The vector of observables X_t contains four variables: detrended GDP (y_t), the term premium factor (χ_t), debt maturity, and the sovereign spread. The state vector S_t collects all variables necessary to describe the economy: the two observable fundamentals (y_t, χ_t), the two unobserved confidence shocks (λ_t, ω_t), and the endogenous variables determined by government policy in the previous period ($b_{S,t}$, $b_{L,t}$).

Following Bocola and Dovis (2019), we set the measurement error variance for y_t and χ_t to zero, so that the filtered path of fundamentals coincides exactly with the data. This leaves two observables (maturity and spreads) and two unobserved shocks (λ_t and ω_t) for the filter to recover. We allow for small measurement errors in maturity and spreads; Appendix D details the algorithm and parameter values.

The filtering procedure delivers, for each period, estimated distributions of the unobserved states. Two objects are of particular interest: the probability of a confidence crisis (λ_t), which governs the government's exposure to a confidence crisis, and the sunspot realization itself (ω_t),

which determines whether the crisis materializes. The model's timing provides an identification scheme that lets the filter separate the two shocks using the observed dynamics of maturity and spreads.

6.2 Spread Decomposition

The main goal is to decompose the observed Italian sovereign spread into components driven by economic fundamentals ($\lambda_t = 0$, $\omega_t = 0$) and by self-fulfilling crises. The *confidence crisis component* is the difference between the spread implemented in the full model and the counterfactual $\omega_t = 0$ and $\lambda = 0$. It captures the effect of confidence risk on the spread of government bonds.

Fundamental dynamics. The filtered fundamental shocks deteriorate during the episode (Figure 6). Italian output falls from 0.04 percent above trend at the start of the sample to -0.04 percent below trend by 2012, reflecting the recessions of 2008–2009 and 2011–2012. The term premium shock χ_t increases during 2008–2009 and again during 2011, consistent with financial stress in the euro zone. As in Bocola and Dovis (2019), these two fundamental forces (the domestic recession and the tightening of global financial conditions) push the government closer to the region where confidence crises become possible and account for the fundamental component of the spread.

Figure 6: Fundamental Shocks During the Italian Crisis

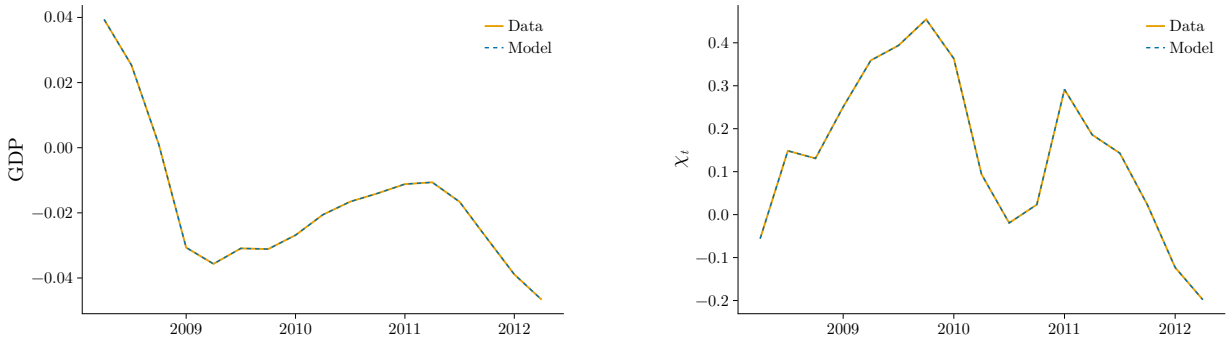

(a) Output

(b) Term Premium Shock

Main result. Confidence risk accounts for approximately 80 percent of the Italian sovereign spread at its late-2011 peak (Figure 7, Panel a). Fundamental risk alone cannot account for the surge. The model also tracks the contemporaneous shortening of debt maturity (Panel b).

Figure 7: Italian Crisis

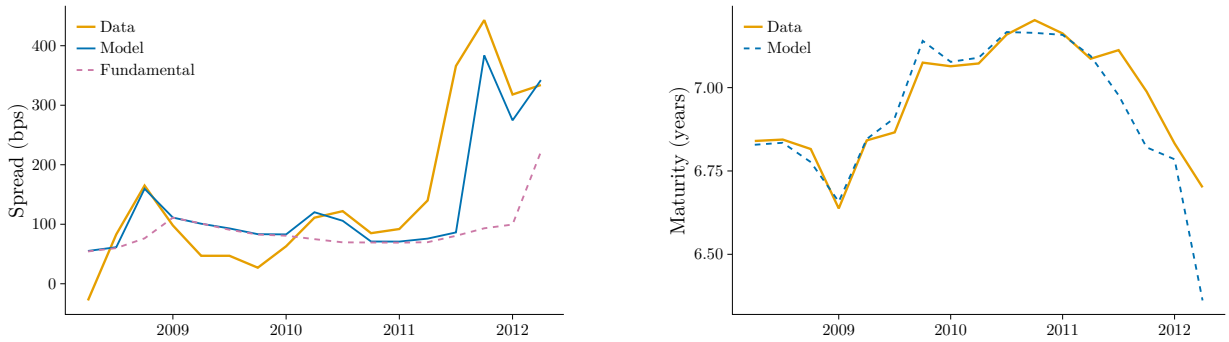

(a) Spread (b) Maturity

Figure 8 displays the filtered paths. Panel (a) shows that the probability of a bad equilibrium fluctuates at moderate levels throughout 2008–2011, then spikes to $\lambda \approx 0.08$ (the grid maximum) at the late-2011/early-2012 peak. Panel (b) shows the filtered probability of the bad sunspot, $P(\omega_t = 1 \mid \text{data})$, which remains near zero throughout the episode, consistent with Italy never defaulting. This confirms that the crisis was one of rising vulnerability rather than coordination in a bad equilibrium.

Figure 8: Sunspot Dynamics

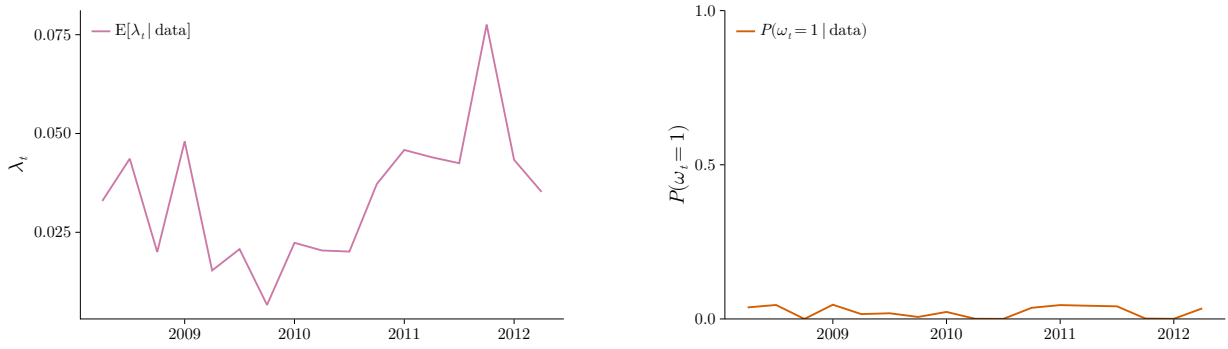

(a) Sunspot Probability (b) Sunspot Realization

Comparison to Bocola–Dovis. Bocola and Dovis (2019) show that dropping maturity from their observables allows their model to attribute a larger share of the 2011 spread spike to rollover risk, but at the cost of predicting that the government should have *lengthened* its maturity by 0.5 years, the opposite of what we observed in the data. The tension arises because, in the Cole–Kehoe framework, higher rollover risk makes long-term debt the insurance instrument. In our model, the mechanism is reversed: higher λ makes short-term debt the insurance instrument, and the government responds by shortening maturity. Our model therefore simultaneously fits

the spread surge and the maturity shortening without any tension between the two observables.

They also find $\omega \approx 0$ throughout the episode, but for a different reason and with different implications. In their Cole–Kehoe framework, a sunspot realization implies immediate default and full market exclusion. Since Italy never defaulted, the bad sunspot was never realized in their model either. As a result, confidence can affect spreads only through a forward-looking pricing of the probability that a future crisis *might* occur. In contrast, in our model the "bad" sunspot might trigger a confidence crisis with low prices for long-term bonds and no default. However, quantitatively, the filter finds a small role for this channel.

Debt dynamics. The filtered portfolio shows long-term debt rising through 2009–2010, short-term debt following a U-shape with a 2011–2012 surge, and total debt-to-GDP overshooting the data in 2009–2010 before converging (Figure 9).

Figure 9: Debt Dynamics

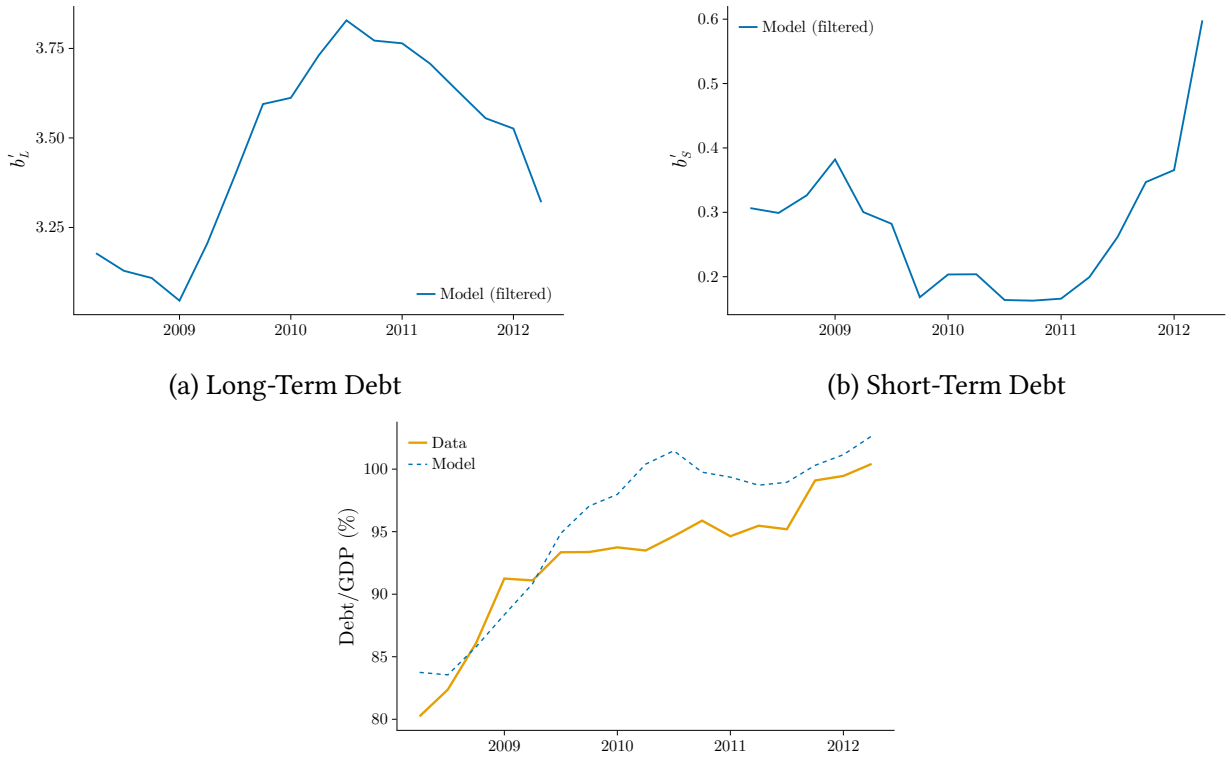

(a) Long-Term Debt

(b) Short-Term Debt

(c) Total Debt/GDP

Panel (a) shows that long-term debt increases through 2009–2010 and then remains elevated before falling in late 2011. Panel (b) shows the U-shaped path for short-term debt: it falls from a local peak in 2009 to a trough around mid-2011 and then surges through the end of the sample.

Panel (c) compares the total debt-to-GDP ratio in the model and the data. The model overshoots the data during 2009–2010 (reaching close to 100 percent of GDP against around 93 percent in the data), then converges to match the data through 2011 and 2012.

The rise in short-term issuance from 2011 to 2012 is consistent with the model's insurance mechanism. As confidence risk (λ) peaked during the episode, the government optimally tilted its portfolio toward short-term debt to reduce its residual exposure on the long-term Laffer curve. The concurrent decline in long-term debt reflects the same rebalancing: as short-term financing expands, the budget needs less long-term issuance to clear.

Finally, we highlight that the filtered debt portfolio is not a calibration target: the particle filter uses maturity and spreads, not total debt or its short-vs-long split. The model's ability to track the observed debt-to-GDP path through 2011–2012 (Panel c) is therefore an untargeted moment.

Sensitivity and robustness. Appendix E reports four diagnostics. First, the bad-equilibrium intersection in Figure 3 sits on a locally upward-sloping segment of the Laffer curve (slope $+0.009$ at the bad root vs $+0.914$ at the good root), confirming the stability and slope asymmetry of Proposition 1. Second, the posterior $5/95$ band on the model spread is tight at most dates and widest at the late-2011 peak (345–474 bps at $2011{:}\mathrm{Q}4$). Third, the headline filtered series are stable across particle count and random seed but sensitive to the measurement-error variances in the H matrix. Fourth, we report an alternative fundamental counterfactual in which the government's portfolio is re-optimized at $\lambda = \lambda_{\min}$ rather than held fixed at the realized policy. This alternative essentially attributes the entire spread to the confidence channel; the gap between it and the headline counterfactual measures the contribution of the maturity-shortening policy response to λ, a margin not present in Bocola and Dovis (2019).

7 Conclusion

This paper revisits the quantitative importance of self-fulfilling risk in the European sovereign debt crisis. We find that shifts in investor beliefs account for approximately 80 percent of Italian sovereign spreads at the late-2011 peak, against the 13 percent that Bocola and Dovis (2019) attribute to confidence risk. The reversal comes from a Calvo-style mechanism in which short-term debt, not long-term debt, is the insurance instrument against price collapses; in this framework, a rising probability of crisis pushes the optimal maturity down rather than up. The same observed maturity shortening that signals low perceived risk in a Cole–Kehoe model signals high perceived risk in ours.

Governments facing fragile market confidence have an active policy lever in debt maturity

management: they can shape their exposure to self-fulfilling crises by shortening maturity when confidence risk rises, not lengthening it. More generally, the quantitative conclusions from self-fulfilling debt models depend on the choice of crisis mechanism: Cole–Kehoe exclusion versus Calvo-style price collapse. The difference is first-order, not stylistic. Extending this framework to monetary unions, where the central bank can affect the laffer curve directly, would allow a structural evaluation of interventions like the ECB's 2012 announcement.

References

Acharya, V. V., Drechsler, I., and Schnabl, P. (2014). A pyrrhic victory? bank bailouts and sovereign credit risk. *Journal of Finance*, 69(6):2689–2739.

Aguiar, M. and Amador, M. (2014). Sovereign debt. In *Handbook of International Economics*, volume 4, pages 647–687. Elsevier.

Aguiar, M. and Amador, M. (2020). Self-fulfilling debt dilution: Maturity and multiplicity in debt models. *American Economic Review*, 110(9):2783–2818.

Aguiar, M., Amador, M., Farhi, E., and Gopinath, G. (2015). Coordination and crisis in monetary unions. *Quarterly Journal of Economics*, 130(4):1727–1779.

Aguiar, M., Amador, M., Hopenhayn, H., and Werning, I. (2019). Take the short route: Equilibrium default and debt maturity. *Econometrica*, 87(2):423–462.

Aguiar, M., Chatterjee, S., Cole, H., and Stangebye, Z. (2016). Quantitative models of sovereign debt crises. In *Handbook of Macroeconomics*, volume 2, pages 1697–1755. Elsevier.

Aguiar, M., Chatterjee, S., Cole, H., and Stangebye, Z. (2022). Self-fulfilling debt crises, revisited. *Journal of Political Economy*, 130(5):1147–1183.

Aguiar, M. and Gopinath, G. (2006). Defaultable debt, interest rates and the current account. *Journal of International Economics*, 69(1):64–83.

Ang, A. and Piazzesi, M. (2003). A no-arbitrage vector autoregression of term structure dynamics with macroeconomic and latent variables. *Journal of Monetary Economics*, 50(4):745–787.

Arellano, C. (2008). Default risk and income fluctuations in emerging economies. *American Economic Review*, 98(3):690–712.

Arellano, C. and Ramanarayanan, A. (2012). Default and the maturity structure in sovereign bonds. *Journal of Political Economy*, 120(2):187–232.

Auclert, A. and Rognlie, M. (2016). Unique equilibrium in the Eaton–Gersovitz model of sovereign debt. *Journal of Monetary Economics*, 84:134–146.

Ayres, J., Navarro, G., Nicolini, J. P., and Teles, P. (2024). Self-fulfilling debt crises with long stagnations. *Staff Report 659, Federal Reserve Bank of Minneapolis*.

Bianchi, J. and Mondragon, J. (2022). Monetary independence and rollover crises. *The Quarterly Journal of Economics*, 137(1):435–491.

Bigio, S., Nuño, G., and Passadore, J. (2023). Debt-maturity management with liquidity costs. *Journal of Political Economy Macroeconomics*, 1(1):119–190.

Bocola, L. (2016). The pass-through of sovereign risk. *Journal of Political Economy*, 124(4):879–926.

Bocola, L., Bornstein, G., and Dovis, A. (2019). Quantitative sovereign default models and the European debt crisis. *Journal of International Economics*, 118:20–30.

Bocola, L. and Dovis, A. (2019). Self-fulfilling debt crises: A quantitative analysis. *American Economic Review*, 109(12):4343–4377.

Bohn, H. (1998). The behavior of u.s. public debt and deficits. *The Quarterly Journal of Economics*, 113(3):949–963.

Broner, F. A., Lorenzoni, G., and Schmukler, S. L. (2013). Why do emerging economies borrow short term? *Journal of the European Economic Association*, 11(suppl_1):67–100.

Brunnermeier, M. K., Garicano, L., Lane, P. R., Pagano, M., Reis, R., Santos, T., Thesmar, D., Van Nieuwerburgh, S., and Vayanos, D. (2016). The sovereign-bank diabolic loop and ESBies. *American Economic Review*, 106(5):508–512.

Calvo, G. A. (1988). Servicing the public debt: The role of expectations. *The American Economic Review*, 78(4):647–661.

Chatterjee, S. and Eyigungor, B. (2012). Maturity, indebtedness, and default risk. *American Economic Review*, 102(6):2674–2699.

Cole, H. L. and Kehoe, T. J. (2000). Self-fulfilling debt crises. *The Review of Economic Studies*, 67(1):91–116.

Conesa, J. C. and Kehoe, T. J. (2017). Gambling for redemption and self-fulfilling debt crises. *Economic Theory*, 64(4):707–740.

Corsetti, G. and Dedola, L. (2016). The mystery of the printing press: Monetary policy and self-fulfilling debt crises. *Journal of the European Economic Association*, 14(6):1329–1371.

De Grauwe, P. and Ji, Y. (2013). Self-fulfilling crises in the Eurozone: An empirical test. *Journal of International Money and Finance*, 34:15–36.

Dvorkin, M., Sánchez, J., Sapriza, H., and Yurdagul, E. (2021). Sovereign debt restructurings. *American Economic Journal: Macroeconomics*, 13(2):26–77.

Eaton, J. and Gersovitz, M. (1981). Debt with potential repudiation: Theoretical and empirical analysis. *Review of Economic Studies*, 48(2):289–309.

Farhi, E. and Tirole, J. (2018). Deadly embrace: Sovereign and financial balance sheets doom loops. *Review of Economic Studies*, 85(3):1781–1823.

Hatchondo, J. C., Martinez, L., and Sosa-Padilla, C. (2016). Debt dilution and sovereign default risk. *Journal of Political Economy*, 124(5):1383–1422.

Krishnamurthy, A., Nagel, S., and Vissing-Jorgensen, A. (2018). ECB policies involving government bond purchases: Impact and channels. *Review of Finance*, 22(1):1–44.

Lorenzoni, G. and Werning, I. (2019). Slow moving debt crises. *American Economic Review*, 109(9):3229–3263.

Niepelt, D. (2014). Debt maturity without commitment. *Journal of Monetary Economics*, 68(S):S37–S54.

Roch, F. and Uhlig, H. (2018). The dynamics of sovereign debt crises and bailouts. *Journal of International Economics*, 114:1–13.

A Proofs

This appendix extends the stylized analysis of Section 4.2 to the full model — stochastic y, χ, λ and endogenous Laffer-curve prices Q_L. In the stylized environment the analytical result follows from primitives because three of the underlying conditions hold by construction (concavity of u, exogenous and positive Q_S, the inequality $Q_L^b < Q_L^g$ that defines the two equilibria). In the full model these are no longer automatic: they become *state-by-state diagnostics* that identify the set of states at which short-term debt acts as insurance. We list these diagnostics, derive the comparative static $\partial b_S^*/\partial\lambda > 0$ under them, and state the analog diagnostic for the Cole–Kehoe region.

Setup. Fix state (s, λ), so the fiscal rule pins down $g = G(b_S, b_L)$ and the state pins down tax revenue τY before the government acts. The government chooses b'_S before the sunspot $\omega \in \{0, 1\}$ is drawn, with $\Pr(\omega = 1) = \lambda$. After ω is realized, b'_L clears the budget at either the good equilibrium $b'_{L,g}(b'_S) \equiv \min \mathbb{B}_L^+(s, \lambda, b'_S)$ or the bad equilibrium $b'_{L,b}(b'_S) \equiv \max \mathbb{B}_L^+(s, \lambda, b'_S)$. The government's payoff is

$$W(\lambda;\, b'_S) = u(g) + \beta \left[(1-\lambda)\, \mathcal{V}(b'_S, b'_{L,g}(b'_S)) + \lambda\, \mathcal{V}(b'_S, b'_{L,b}(b'_S))\right], \tag{24}$$

where $\mathcal{V}(b'_S, b'_L) \equiv \mathbb{E}_{y',\chi',\lambda'}\left[V(b'_S, b'_L, y', \chi', \lambda')\right]$ is the next-period continuation value as a function of the inherited debt portfolio, integrating out the exogenous shocks at the model's equilibrium policy.

State-by-state diagnostics for the insurance channel. The following four quantities are computable at any state $(s, \lambda, b_S, b_L, b'_S)$ in the calibrated model:

(i) Concavity of the continuation value in long-term debt: $\partial^2\mathcal{V}/\partial(b'_L)^2 \le 0$;

(ii) Positive marginal revenue from short-term issuance: $\partial\mathcal{L}/\partial b'_S > 0$, where

$$\frac{\partial \mathcal{L}}{\partial b'_S} = Q_S + b'_S \frac{\partial Q_S}{\partial b'_S} + \left(b'_L - (1-\delta) b_L\right) \frac{\partial Q_L}{\partial b'_S}; \tag{25}$$

(iii) Slope asymmetry on the Laffer curve: $\mathcal{L}'(b'_{L,b}) < \mathcal{L}'(b'_{L,g})$ (the bad root sits on the flat part of the recovery branch);

(iv) Dominance of the within-period insurance channel over the cross-period rollover channel: $\Delta_{\text{within}} + \Delta_{\text{cross}} \ge 0$, where

$$\Delta_{\text{within}} \equiv \mathcal{V}_{b_L}(b'_S, b'_{L,b}) \frac{\partial b'_{L,b}}{\partial b'_S} - \mathcal{V}_{b_L}(b'_S, b'_{L,g}) \frac{\partial b'_{L,g}}{\partial b'_S},$$
$$\Delta_{\text{cross}} \equiv \mathcal{V}_{b_S}(b'_S, b'_{L,b}) - \mathcal{V}_{b_S}(b'_S, b'_{L,g}).$$

Proposition 2 (Sufficient diagnostics for the insurance comparative static, full model)**.** *Suppose the state (s, λ) lies in the multiplicity region $\mathcal{S}_M$ for the relevant range of b'_S, so that both equilibria coexist, and that diagnostics (i)–(iv) hold at that state. Then $\partial^2 W / \partial\lambda\, \partial b'_S > 0$, and the optimal short-term debt level $b^*_S(\lambda) \equiv \arg\max_{b'_S} W(\lambda;\, b'_S)$ is locally increasing in λ.*

In the stylized environment of Section 4.2, diagnostics (i)–(iii) hold by construction or reduce to the primitive parameter restriction (**??**) on $\beta, \kappa_L, \tilde{\nu}, \delta$. Only (iv) is a substantive restriction on the continuation value. In the full model with stochastic shocks and endogenous prices, none of (i)–(iv) hold by construction. Section 5 reports their numerical evaluation at every filtered Italian state.

Proof of Proposition 1. We first derive the stationary equilibrium prices in closed form. The short bond is auctioned at time t before ω_t is drawn and pays $1 + \kappa_S$ at $t+1$ if the government does not default, with the per-unit recovery $\tilde{\nu}$ otherwise. In the stationary equilibrium of the stylized environment the bad sunspot $\omega = 1$ triggers default with the bond settling at the recovery floor, so the unconditional next-period default probability equals λ. Lenders therefore price the short bond at the expected discounted payoff,

$$Q_S \;=\; \beta\big[(1-\lambda)(1+\kappa_S) \;+\; \lambda\,\tilde{\nu}\big], \tag{26}$$

which gives (23). The bad-sunspot long-bond price satisfies (21); the good-sunspot pricing equation (22) is linear in Q^g_L and yields the closed form

$$Q^g_L(\lambda) \;=\; \frac{\beta(1-\lambda)\kappa_L \;+\; \beta\lambda\,\tilde{\nu}}{1 \;-\; \beta(1-\lambda)(1-\delta)}. \tag{27}$$

Under (**??**), $Q^g_L(\lambda) > \tilde{\nu} = Q^b_L$ for every $\lambda \in [0,1]$. The three prices Q_S, Q^g_L, Q^b_L are constants in b'_S at the stationary equilibrium: a marginal deviation in b'_S does not alter the stationary equilibrium at which they are evaluated. Differentiation of the period budget identity therefore gives $\partial b'_L(\omega)/\partial b'_S = -Q_S/Q^\omega_L$. The government's first-order condition at the stationary policy b^*_S is

$$(1-\lambda)\Big[\mathcal{V}_{b_S}(b^*_S, b^g_L) - \tfrac{Q_S}{Q^g_L}\,\mathcal{V}_{b_L}(b^*_S, b^g_L)\Big] + \lambda\Big[\mathcal{V}_{b_S}(b^*_S, b^b_L) - \tfrac{Q_S}{\tilde{\nu}}\,\mathcal{V}_{b_L}(b^*_S, b^b_L)\Big] \;=\; 0. \tag{28}$$

Differentiating (28) with respect to λ at the optimum decomposes the cross-partial $\partial^2 W/(\partial\lambda\,\partial b'_S)$ into three terms. The first is the weight effect, $\big[\mathcal{V}_{b_S}(b^*_S, b^b_L) - \frac{Q_S}{\tilde{\nu}}\mathcal{V}_{b_L}(b^*_S, b^b_L)\big] - \big[\mathcal{V}_{b_S}(b^*_S, b^g_L) - \frac{Q_S}{Q^g_L}\mathcal{V}_{b_L}(b^*_S, b^g_L)\big]$, which captures the difference in marginal benefit across the two sunspot states; under the price asymmetry (**??**) and $\mathcal{V}_{b_L} < 0$ (Lemma 1), the term $-Q_S\mathcal{V}_{b_L}/Q^\omega_L$ is larger at the bad sunspot, so the weight effect is positive. The second is the price effect: differentiating (27) yields

$$\frac{\partial Q^g_L}{\partial\lambda} \;=\; \frac{\beta(\tilde{\nu}-\kappa_L)\big[1-\beta(1-\lambda)(1-\delta)\big] - \beta(1-\delta)\big[\beta(1-\lambda)\kappa_L + \beta\lambda\tilde{\nu}\big]}{\big[1-\beta(1-\lambda)(1-\delta)\big]^2} \;<\; 0$$

under (??), so $1/Q_L^g$ is increasing in λ and the magnitude of the good-state insurance term $-Q_S \mathcal{V}_{b_L}(b_S^*, b_L^g)/Q_L^g$ rises with λ. This effect is strictly positive. The third is the cross-period effect, $\mathcal{V}_{b_S}(b_S^*, b_L^b) - \mathcal{V}_{b_S}(b_S^*, b_L^g)$, whose sign is governed by the cross-partial $\mathcal{V}_{b_S b_L}$; under $\mathcal{V}_{b_S b_L} \leq 0$ and $b_L^b > b_L^g$, this effect is non-positive. Condition (iv) bounds the magnitude of the cross-period effect, so the sum of the three effects is strictly positive, $\partial^2 W/(\partial\lambda\, \partial b_S') > 0$. Topkis's theorem delivers $\partial b_S^*/\partial\lambda > 0$.

We next establish a property of the continuation value used in the proof of the full-model proposition.

Lemma 1 (Monotonicity of the continuation value)**.** *Under the paper's primitives (CRRA utility, fiscal rule $G(b_S, b_L) = \bar{g} - \alpha_1 \max(b_S + b_L - \bar{b}, 0)$, default rule with autarky spending $g_D < \tau Y_{\min}$, and pari-passu recovery $\tilde{v} = \phi(\tau Y' - g_D)/(b_S' + b_L'))$, the continuation value satisfies $\mathcal{V}_{b_L}(b_S', b_L') < 0$ for all $b_L' > 0$.*

Proof. The continuation value $\mathcal{V}(b_S', b_L')$ is the expected next-period-and-beyond welfare from inheriting the portfolio (b_S', b_L'), holding all other states fixed and integrating out the exogenous shocks at the model's equilibrium policy. Raising b_L' enters the next-period problem through three channels, each of which weakly reduces welfare:

(a) Debt service. The coupon payment $\kappa_L b_L'$ scales linearly with b_L', tightening the next-period budget constraint (5). Holding all else fixed, this requires either lower g' or higher new issuance, both of which reduce welfare.

(b) Fiscal rule. When total inherited debt exceeds $\bar{b}$, the fiscal rule reduces g' at rate α_1 in b_L'. Since $u'(g) = g^{-\sigma} > 0$ under CRRA, $u(g')$ strictly falls. This channel is silent for $b_S' + b_L' \leq \bar{b}$ but does not change sign there.

(c) Default probability. Higher b_L' enters the period-$t+1$ deficit linearly through the coupon obligation $\kappa_L b_L'$, shrinking the set of states $(Y_{t+1}, \chi_{t+1}, \lambda_{t+1})$ for which the Laffer curve admits a stable budget-clearing root. The probability of default $\Pr(d' = 1)$ is therefore weakly increasing in b_L'. Default delivers period payoff $u(g_D) < u(\tau Y') \leq u(g')$, since $g_D < \tau Y_{\min}$ by construction; the per-period payoff under default is strictly less than the per-period payoff in any non-default state. The expected per-period utility is therefore strictly decreasing in b_L' through the default-probability channel, independent of any comparison between V_{def} and the no-default continuation value.

At any $b_L' > 0$, channels (a) and (c) operate strictly, so $\mathcal{V}_{b_L}(b_S', b_L') < 0$ holds at any state where the no-default continuation does not over-compensate for the period-payoff drop via the debt-discharge effect. Section 5 verifies this inequality, together with the four conditions of Proposition 2, at every filtered Italian quarter. □

Proof of Proposition 2. Since both roots lie on upward-sloping portions of $\mathcal{L}$ (stable equilibria), $\mathcal{L}'(b_{L,\omega}') > 0$ for $\omega \in \{g, b\}$. The implicit function theorem on $\mathcal{L}(s, \lambda, b_S', b_{L,\omega}'(b_S')) = g - \tau Y$ gives

$$\frac{\partial b_{L,\omega}'}{\partial b_S'} = -\frac{\partial \mathcal{L}/\partial b_S'}{\mathcal{L}'(b_{L,\omega}')} < 0,$$

where the sign uses condition (ii). By condition (iii), $\mathcal{L}'(b'_{L,b}) < \mathcal{L}'(b'_{L,g})$, so

$$\left|\frac{\partial b'_{L,b}}{\partial b'_S}\right| > \left|\frac{\partial b'_{L,g}}{\partial b'_S}\right| :$$

a marginal increase in b'_S reduces the bad-equilibrium debt stock by more than the good-equilibrium stock.

Differentiating $W(\lambda; b'_S) = u(g) + \beta\big[(1-\lambda)\mathcal{V}(b'_S, b'_{L,g}(b'_S)) + \lambda\mathcal{V}(b'_S, b'_{L,b}(b'_S))\big]$ with respect to b'_S gives

$$\begin{aligned}\frac{\partial W}{\partial b'_S} = \beta\Big\{&(1-\lambda)\Big[\mathcal{V}_{b_S}(b'_S, b'_{L,g}) + \mathcal{V}_{b_L}(b'_S, b'_{L,g})\,\tfrac{\partial b'_{L,g}}{\partial b'_S}\Big] \\ &+ \lambda\Big[\mathcal{V}_{b_S}(b'_S, b'_{L,b}) + \mathcal{V}_{b_L}(b'_S, b'_{L,b})\,\tfrac{\partial b'_{L,b}}{\partial b'_S}\Big]\Big\}.\end{aligned}$$

Taking the derivative with respect to λ and collecting terms,

$$\frac{\partial^2 W}{\partial\lambda\,\partial b'_S} = \beta\big(\Delta_{\text{within}} + \Delta_{\text{cross}}\big),$$

with

$$\Delta_{\text{within}} = \mathcal{V}_{b_L}(b'_S, b'_{L,b})\,\tfrac{\partial b'_{L,b}}{\partial b'_S} - \mathcal{V}_{b_L}(b'_S, b'_{L,g})\,\tfrac{\partial b'_{L,g}}{\partial b'_S}, \quad \Delta_{\text{cross}} = \mathcal{V}_{b_S}(b'_S, b'_{L,b}) - \mathcal{V}_{b_S}(b'_S, b'_{L,g}).$$

The two pieces correspond to the two channels through which a marginal b'_S affects welfare differently in the bad versus good equilibrium: Δ_{within} captures the within-period insurance channel (the implicit-function chain through b'_L), and Δ_{cross} captures the cross-period rollover channel (the direct dependence of $\mathcal{V}$ on inherited short-term debt).

Signing Δ_{within}. Substituting the implicit-function expressions,

$$\Delta_{\text{within}} = \frac{\partial\mathcal{L}}{\partial b'_S}\left[\frac{-\mathcal{V}_{b_L}(b'_S, b'_{L,b})}{\mathcal{L}'(b'_{L,b})} - \frac{-\mathcal{V}_{b_L}(b'_S, b'_{L,g})}{\mathcal{L}'(b'_{L,g})}\right].$$

The prefactor is positive by condition (ii). By Lemma 1, $-\mathcal{V}_{b_L}(b'_S, b'_{L,\omega}) > 0$. Since $b'_{L,b} > b'_{L,g}$, condition (i) (concavity in b_L) implies $-\mathcal{V}_{b_L}(b'_S, b'_{L,b}) \geq -\mathcal{V}_{b_L}(b'_S, b'_{L,g})$. Combined with $1/\mathcal{L}'(b'_{L,b}) > 1/\mathcal{L}'(b'_{L,g})$ from condition (iii), the bracketed expression is non-negative, so $\Delta_{\text{within}} \geq 0$ with strict inequality under strict versions of (i)–(iii).

Total cross-partial. Condition (iv) states $\Delta_{\text{within}} + \Delta_{\text{cross}} \geq 0$, with strict inequality under strict (i)–(iv). Hence $\partial^2 W/(\partial\lambda\,\partial b'_S) > 0$, and Topkis's theorem implies $\partial b^*_S(\lambda)/\partial\lambda > 0$. □

Remark 1 (Sign of the cross-period channel)**.** *The direct cross-period term Δ_{cross} depends on $\mathcal{V}_{b_S b_L}$, the cross-partial of the continuation value in (b_S, b_L). In sovereign-default models with non-trivial default risk, more inherited long-term debt typically amplifies the marginal cost of inherited short-*

term debt, so $\mathcal{V}_{b_S b_L} \leq 0$ *and hence* $\Delta_{\text{cross}} \leq 0$. *The cross-period channel therefore partially offsets the within-period insurance channel. Condition (iv) requires the within-period channel to dominate; Section 5 verifies numerically that this dominance holds over the calibrated parameter region.*

B Computational Algorithm

We solve the model by value function iteration on the discretized state space $(b_S, b_L, y, \chi, \lambda)$, combining grid-based Laffer curve classification with logit-smoothed policy functions following Dvorkin et al. (2021).

Grids and Initialization

Output y and the SDF state χ are each discretized by Tauchen (1986) and combined into a joint Markov chain via Gaussian quadrature, producing transition matrix $\Pi_{y\chi}$ and conditional SDF weights $\{M_{ij}\}$. The confidence shock λ is discretized on a uniform grid over $[\lambda_{\min}, \lambda_{\max}]$ with an AR(1) Tauchen-style transition matrix Π_λ. A fine evaluation grid $b_{L,\text{eval}} \in [0, \bar{b}_L]$ of 500 points is used only for Laffer curve evaluation; equilibrium debt levels are stored and interpolated on the coarser b_L state grid.

The value function is initialized at the no-default steady state, $V^0 = u(\bar{g})/(1-\beta)$. Bond prices use a recovery-based initialization, $Q_L^0(b_L') = \min\big(Q_L^{\text{rf}},\ \phi(\tau Y - g_D)/b_L'\big)$. This seeds the declining $Q_L(b_L')$ profile needed for the Laffer curve to exhibit a second hump from the first iteration. Short-term prices are initialized at their risk-free values, $Q_S^0 = Q_S^{\text{rf}}$.

Pre-Logit Value and Choice Probabilities

For each state $(s, \lambda) = (b_S, b_L, y, \chi, \lambda)$ and candidate b_S', define

$$W(s, \lambda, b_S') = (1-\lambda)\big[u(\tilde{g}_0) + \beta\, \mathbb{E}_{y',\chi',\lambda'} V(s_g', \lambda')\big] + \lambda\big[u(\tilde{g}_1) + \beta\, \mathbb{E}_{y',\chi',\lambda'} V(s_b', \lambda')\big], \tag{29}$$

where $\tilde{g}_\omega = g$ if the ω-branch repays and $\tilde{g}_\omega = g_D$ if it defaults, and $s_g' = (b_S', b_{L,g}^*, y', \chi')$ and $s_b' = (b_S', b_{L,b}^*, y', \chi')$ are next-period states under each sunspot. Choice probabilities and the value function are computed using a numerically stable logit, where $\rho > 0$ is the taste-shock variance:

$$\Pr(b_S' = b_{S,k}' \mid s, \lambda) = \frac{\exp\big((W_k - \bar{W})/\rho\big)}{\sum_j \exp\big((W_j - \bar{W})/\rho\big)}, \qquad V(s, \lambda) = \bar{W} + \rho \log \sum_j \exp\Big(\tfrac{W_j - \bar{W}}{\rho}\Big), \tag{30}$$

where $\bar{W} = \max_j W_j$.

Algorithm

Each outer iteration proceeds as follows.

1. **Laffer curve classification.** For each state $(b_S, b_L, y, \chi, \lambda)$ and each candidate b_S', compute the financing need $\Delta = g - \tau Y + (1+\kappa_S) b_S + \kappa_L b_L$ and evaluate

$$\mathcal{L}(b_L') = Q_L(y, \chi, \lambda, b_S', b_L') \cdot (b_L' - (1-\delta) b_L) + \bar{Q}_S \cdot b_S'$$

on the fine grid, where $\bar{Q}_S = (1-\lambda)Q_S(b^*_{L,g}) + \lambda Q_S(b^*_{L,b})$ is the previous-iteration equilibrium-weighted short-term price (since lenders price Q_S before the sunspot is drawn). Identify stable crossings where $\mathcal{L}$ crosses Δ from below. Cases 2, 3, 4 below correspond to $\mathcal{S}_U, \mathcal{S}_{CK}, \mathcal{S}_M$ in Section 4; Case 1 (no equilibrium) is captured by the default rule (16).

- **Case 1 (Fundamental default):** No stable crossings: both sunspots default.
- **Case 2 (Unique equilibrium):** One stable crossing and $\mathcal{L}(\bar{b}_L) \geq \Delta$: both sunspots select the same root; ω is irrelevant.
- **Case 3 (Cole–Kehoe):** One stable crossing and $\mathcal{L}(\bar{b}_L) < \Delta$: good sunspot repays at the unique root; bad sunspot defaults.
- **Case 4 (LW multiplicity):** Two or more stable crossings and $\mathcal{L}(\bar{b}_L) \geq \Delta$: good sunspot selects the lowest root ($b^*_{L,g}$), bad sunspot selects the highest ($b^*_{L,b}$).

2. **Value function update.** Compute $W(s, \lambda, b'_S)$ for all b'_S candidates, then update V and $\Pr(b'_S)$ via (30).

3. **Price updates.** Update Q_L and Q_S from the no-arbitrage conditions (19)–(20), integrating over the current logit probabilities. For Q_L, we evaluate continuation prices at the previous-iteration Q_L following Chatterjee and Eyigungor (2012).

4. **Damped accumulator.** A damped accumulator Q^{main} is updated each iteration via $Q^{\text{main}} \leftarrow (1-\epsilon)Q^{\text{main}} + \epsilon Q^{\text{new}}$ with damping factor $\epsilon = 0.05$, following Chatterjee and Eyigungor (2012). Convergence is checked on Q^{main}: the algorithm stops when $\|Q_L^{\text{main}} - Q_L^{\text{prev}}\|_\infty$, $\|Q_S^{\text{main}} - Q_S^{\text{prev}}\|_\infty$, and $\|V^{\text{main}} - V^{\text{prev}}\|_\infty$ all fall below 10^{-5}.

C Empirical Definitions

Maturity. The portfolio maturity is a face-value-weighted average of the maturities of the two instruments. Short-term bonds have maturity 1 (one quarter). Long-term bonds have risk-free Macaulay duration $1/\delta$ (quarters). We use risk-free duration to isolate changes in quantities from movements in bond prices. Dividing by 4 converts to annual years:

$$\text{mat}_t = \frac{b'_S \cdot 1 + b'_L \cdot (1/\delta)}{4\,(b'_S + b'_L)}.$$

Spreads. The short-term spread is the excess gross return of the sovereign bond over the risk-free short rate:

$$s_S = 400 \times \left(\frac{1+\kappa_S}{q_S} - R_{f,S} \right),$$

where $(1+\kappa_S)/q_S$ is the sovereign gross return and $R_{f,S}$ is the state-dependent risk-free gross return. The long-term spread is the excess yield-to-maturity over the risk-free long yield:

$$s_L = 400 \times (\text{YTM}_L - R_{f,L}), \qquad \text{YTM}_L = \frac{\kappa_L}{q_L} - \delta.$$

Both are in annualized percentage points (multiply by 100 to convert to basis points). The portfolio spread is a market-value-weighted average:

$$s = \frac{q_S b'_S \cdot s_S + q_L b'_L \cdot s_L}{q_S b'_S + q_L b'_L}.$$

D Particle Filter

We cast the model as a nonlinear state-space system and estimate the unobserved states using a bootstrap Sequential Monte Carlo (particle) filter. This appendix describes the state vector, measurement equation, and algorithm.

State Vector and Observables

The state vector is $S_t = (y_t, \chi_t, \lambda_t, \omega_t, b_{S,t}, b_{L,t})$. The fundamentals (y_t, χ_t) are observed directly from the data and assigned zero measurement error, so filtered values coincide exactly with the data series. The confidence shocks (λ_t, ω_t) and the debt stocks $(b_{S,t}, b_{L,t})$ are latent and recovered by the filter.

The observables are portfolio maturity and the sovereign spread. The measurement equation is

$$\begin{pmatrix} \text{maturity}_t \\ \text{spread}_t \end{pmatrix} = \begin{pmatrix} \hat{m}(S_t) \\ \hat{s}(S_t) \end{pmatrix} + \eta_t, \qquad \eta_t \sim \mathcal{N}(0, H^{-1}),$$

where $\hat{m}$ and $\hat{s}$ are the model-implied maturity and spread evaluated at state S_t via interpolation of the solved policy and price functions, and H is the 2×2 precision matrix for measurement errors. We set the measurement error standard deviations to $\sigma_{\text{maturity}} = 0.05$ years and $\sigma_{\text{spread}} = 0.08$ (in model units, where $1.0 = 100$ bps), with zero correlation.

Initialization

We initialize $N = 50{,}000$ particles at $t = 1$. The initial debt portfolio $(b_{S,0}, b_{L,0})$ is recovered from the first observation using observed maturity (m_0) and total debt-to-GDP (d_0), exploiting the identity

$$m_0 = \frac{b_{S,0} \cdot 1 + b_{L,0} \cdot (1/\delta)}{b_{S,0} + b_{L,0}}, \qquad b_{S,0} + b_{L,0} = d_0/(4 \cdot e^{y_0}).$$

Each particle draws $b^k_{S,0} \sim \mathcal{N}(b_{S,0}, 0.05^2)$ and $b^k_{L,0} \sim \mathcal{N}(b_{L,0}, 0.10^2)$, clamped to the grid bounds. The confidence shock is initialized as $\lambda^k_0 \sim \text{Uniform}[\lambda_{\min}, \lambda_{\max}]$ and $\omega^k_0 \sim \text{Bernoulli}(0.5)$.

Algorithm

For each period $t = 1, \ldots, T$:

1. **Set fundamentals.** Set $y^k_t = y_t$ and $\chi^k_t = \chi_t$ for all particles, taken directly from the data.
2. **Propagate confidence shocks.** For each particle k, draw λ^k_t from the Markov transition Π_λ using the previous period's resampled λ^k_{t-1} as the current state. Then draw $\omega^k_t \sim \text{Bernoulli}(\lambda^k_t)$.

3. **Evaluate policies and prices.** For each particle, interpolate the government's short-term debt choice $b'^k_{S,t}$ from the logit choice distribution at state S^k_t, and the corresponding long-term debt $b'^k_{L,t}$ from the equilibrium debt rule conditional on ω^k_t. Compute model-implied maturity $\hat{m}^k_t$ and spread $\hat{s}^k_t$ using interpolated price functions.

4. **Compute weights.** Particles in default receive weight zero. For repaying particles, the unnormalized weight is the Gaussian likelihood

$$\tilde{w}^k_t = \exp\left(-\tfrac{1}{2}\begin{pmatrix}\hat{m}^k_t - m_t\\ \hat{s}^k_t - s_t\end{pmatrix}^\top H \begin{pmatrix}\hat{m}^k_t - m_t\\ \hat{s}^k_t - s_t\end{pmatrix}\right).$$

Normalize to obtain $w^k_t = \tilde{w}^k_t / \sum_j \tilde{w}^j_t$. If the effective sample size $\mathrm{ESS}_t = 1/\sum_k (w^k_t)^2$ falls below $0.01\,N$, we replace the likelihood weights with an inverse-distance scheme to prevent particle collapse. Specifically, let $\Delta^k_t = (\hat{m}^k_t - m_t,\ \hat{s}^k_t - s_t)^\top$ denote the period-t observation residual for particle k, and define the Mahalanobis distance

$$d^k_t \;\equiv\; (\Delta^k_t)^\top H\, \Delta^k_t,$$

using the same precision matrix H as in the likelihood. The fallback weights are

$$\tilde{w}^k_t \;=\; \left(d^k_t + \varepsilon\right)^{-\zeta},$$

with $\zeta = 5.5$ and $\varepsilon = 10^{-9}$ for numerical regularization, then normalized to sum to one. The fallback fires only in the rare quarters where the likelihood collapses below the $0.01\,N$ ESS threshold (typically 1–2 quarters at the height of the crisis); in all other periods the standard likelihood weighting applies.

5. **Resample.** Apply systematic resampling to obtain N equally weighted particles. Carry forward the resampled λ^k_t for the Markov transition in the next period.

6. **Propagate debt.** Set $b^k_{S,t+1} = b'^k_{S,t}$ and $b^k_{L,t+1} = b'^k_{L,t}$ for the next period. Defaulted particles re-enter with debt at the grid minimum.

Spread Decomposition

At each particle and period, we compute three model-implied spreads corresponding to the decomposition in Section 6. All three use the same realized state $(y_t, \chi_t, b_{S,t}, b_{L,t})$ and the same $b'_{S,t}$ draw, so differences reflect only the pricing of confidence risk.

- **Fundamental spread**: prices evaluated at $\lambda = \lambda_{\min}$ and $\omega = 0$, shutting down both confidence margins.

- **Fundamental + confidence spread**: prices evaluated at the filtered λ_t^k but with $\omega = 0$. This is the cumulative level combining both the fundamental and confidence-risk components; the confidence-risk component alone is the difference between this spread and the fundamental spread.
- **Realized spread**: prices evaluated at the realized $(\lambda_t^k, \omega_t^k)$, matching the full model prediction.

We compute period-t aggregate values as weighted averages $\sum_k w_t^k \cdot (\cdot)^k$ across particles.

E Sensitivity and Robustness

This appendix collects four diagnostics that probe the central quantitative results of Section 6. All four are produced by a single script (`run_sensitivity.jl`) using the baseline calibration and filter output.

Bad-equilibrium slope on the calibrated Laffer curve

Proposition 2 condition (iii) requires the Laffer curve to be flatter at the bad equilibrium than at the good equilibrium, with both intersections on locally increasing segments. Evaluating the curve plotted in Figure 3 at the low-b'_S value where the multiplicity occurs ($b'_S = 0.273$, Case 4), we find $\mathcal{L}'(b'_{L,g}) = +0.914$ at the good root and $\mathcal{L}'(b'_{L,b}) = +0.009$ at the bad root. Both slopes are strictly positive (stable equilibria), and the bad-root slope is two orders of magnitude smaller (the slope asymmetry of Proposition 2 (iii)).

Posterior uncertainty on the model spread

Figure 10 reports the weighted 5th, 50th, and 95th percentiles of the model spread across the particle swarm at each filtered quarter. The band is tight at most dates and widest at the late-2011 peak, ranging from 345 to 474 bps at 2011:Q4 against an observed value of 443 bps.

Figure 10: Posterior 5/95 bands on the model spread

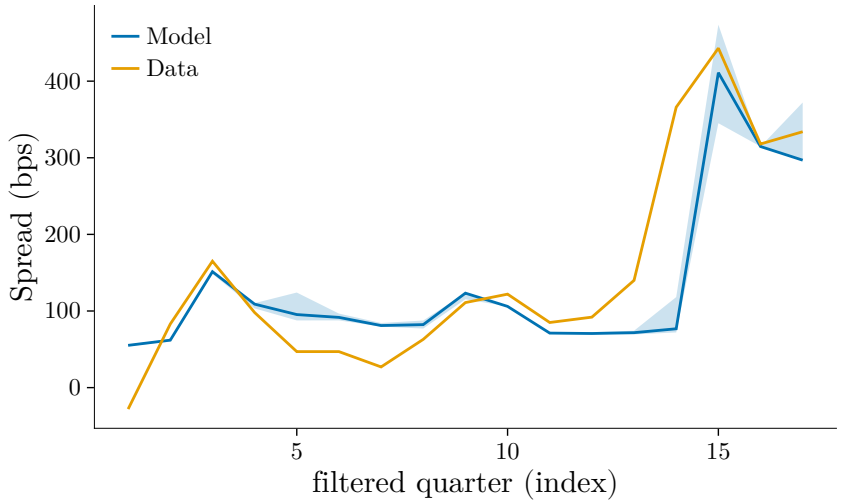

Notes: Weighted 5th, 50th, and 95th percentiles of the model-spread distribution across the particle swarm at each filtered quarter, $N = 50{,}000$ particles. Shaded region is the 5/95 band; solid line is the median. The observed Italian spread is overlaid in amber.

Filter robustness to particle count and measurement error

Table 3 reports three summary statistics under perturbations to the particle count N, the maturity and spread measurement-error standard deviations σ_{mat} and σ_{spr}, and the random seed. The peak filtered λ, the average ω, and the peak model spread are all stable across particle counts (20,000 to 100,000) and seeds. Doubling either measurement-error variance moves the peak model spread by ±100 bps, identifying the H matrix as the most consequential filter choice.

Table 3: Filter sensitivity

Configuration	λ_{peak}	$\bar{\omega}$	$\text{spread}_{\text{peak}}$ (bps)
Baseline ($N = 50{,}000$, $\sigma_{\text{mat}} = 0.04$, $\sigma_{\text{spr}} = 0.08$)	0.054	0.026	269
$N = 20{,}000$	0.055	0.026	265
$N = 100{,}000$	0.061	0.023	262
σ_{mat} doubled	0.054	0.022	363
σ_{spr} doubled	0.050	0.030	164
Alternative random seed	0.054	0.026	273

Alternative fundamental counterfactual: re-optimized policy at $\lambda = \lambda_{\min}$

The fundamental component reported in Section 6 follows Bocola and Dovis (2019): it holds the realized portfolio (b'_S, b'_L) fixed and re-prices the bond at $\lambda = \lambda_{\min}$. In their setting this construction isolates the

pricing channel of confidence risk because the government has no portfolio margin to respond to λ. In our setting the government does respond by shortening maturity, so the realized portfolio embeds a confidence-driven policy choice. The Bocola–Dovis construction therefore attributes part of the policy-response effect to the fundamental component.

Figure 11 compares two specifications:

- **Specification A** (the headline fundamental in Section 6): same realized portfolio, priced at $\lambda_{\min}$.
- **Specification B**: re-optimized portfolio at $\lambda_{\min}$ (the government chooses b'_S as if confidence risk were absent), priced at $\lambda_{\min}$.

Specification B averages 0.3 bps over the sample and reaches 0.3 bps at the late-2011 peak, against 96 bps and 195 bps respectively under Specification A. The full gap between the model spread and Specification B — essentially the entire spread, including the part Specification A labels fundamental — is attributable to the joint pricing and policy responses to confidence risk. The gap between Specifications A and B isolates the portion driven by the maturity-shortening policy response. Within our model, this is a substantive contribution of the framework over Bocola and Dovis (2019): the maturity instrument is itself a transmission channel of λ, not merely a passive observable used to identify it.

Figure 11: Counterfactual specifications for the fundamental component

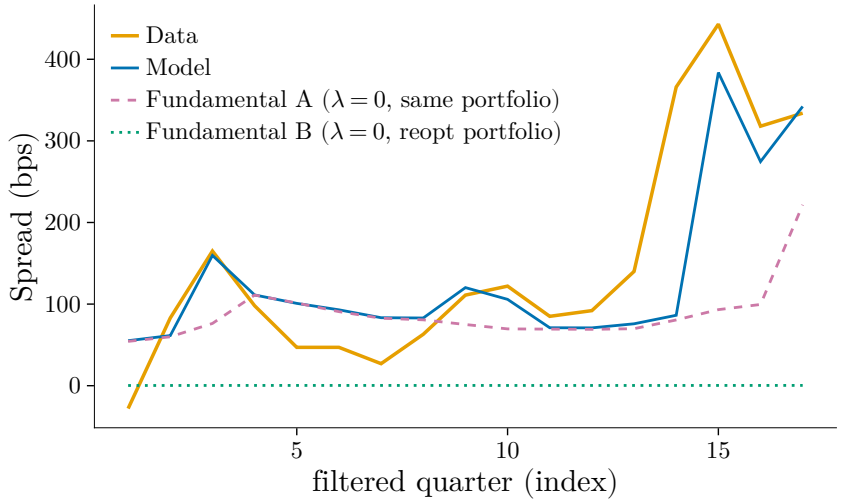

Notes: Data (amber), realized model spread (blue), Specification A (reddish-purple dashed; same portfolio, priced at $\lambda_{\min}$), Specification B (green dotted; re-optimized portfolio at $\lambda_{\min}$, priced at $\lambda_{\min}$). All quantities in basis points.